Wide Band and Wide Field Imaging - I

Urvashi Rau, NRAO

Sixteenth Synthesis Imaging Workshop
16-23 May 2018

NRAO ALMA AUI NSF New Mexico Tech SCIENCE · ENGINEERING · RESEARCH · UNIVERSITY The University of New Mexico New Mexico CONSORTIUM

2D Fourier Transform

Sky Brightness

Visibilities

Point Spread Function

Convolution

CLEAN

Deconvolution

Weighting

Non-coplanar baselines

Dynamic Range

W-term

Not a 2D Fourier Transform

Multi-Frequency Synthesis

Gridding

Antenna Power pattern

Mosaics

Pointings

Primary Beams

Polarization

Field of View

Synthesized Beam

Short spacings

Major Cycles

Angular Resolution

Minor Cycles

Basic Calibration and Imaging

An interferometer partially measures the spatial Fourier transform of the sky brightness distribution.

$$V_{ij}^{obs}(\nu,t) = \boxed{M_{ij}(\nu,t)} S_{ij}(\nu,t) \iint I(l,m) e^{2\pi i (ul+vm)} dl\, dm$$

Observed visibilities (Data)

Direction Independent Gains

UV sampling pattern

Sky Brightness (Image)

Fourier transform kernel

$$I^{obs}(l,m) = I^{PSF}(l,m) * I^{sky}(l,m)$$

Standard calibration eliminates $M_{ij}(\nu,t)$

The observed image is a convolution of the PSF with the sky brightness.

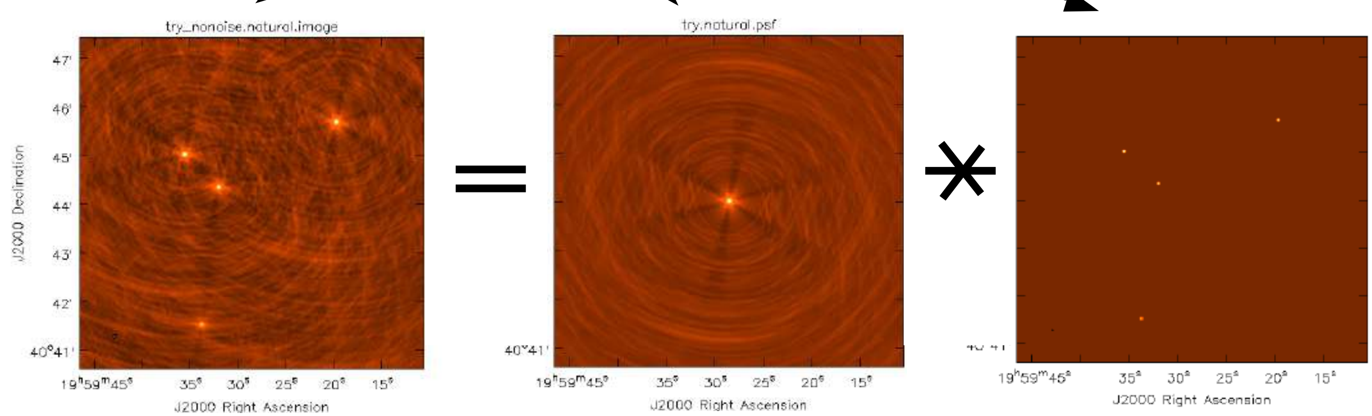

Wide Band and Wide-Field Imaging

An interferometer partially measures the spatial Fourier transform of the sky brightness distribution.

$$V_{ij}^{obs}(\nu,t) \approx M_{ij}(\nu,t) S_{ij}(\nu,t) \iint I(l,m) e^{2\pi i(ul+vm)} dl\, dm$$

$$V_{ij}^{obs}(\nu,t) = M_{ij}(\nu,t) S_{ij}(\nu,t) \iiint M_{ij}^{s}(l,m,\nu,t) I(l,m,\nu,t) e^{2\pi i(ul+vm+w(n-1))} dl\, dm\, dn$$

Direction Independent Gains

- Eliminated during calibration

Primary Beams

- Power pattern varies with time, frequency and baseline

Sky-brightness varies with frequency (time)

- All sources have spectral structure (some vary with time)

W-Term

-Non-coplanar baselines

-Sky curvature

Direction Dependent Effects

=> The observed image is NOT a simple convolution equation

Wide Band Imaging

(sky and instrument change with frequency)

Wide Field Imaging

(non-coplanar baselines and the W-term)

Full Beam Imaging

(antenna primary beams)

Sky and Instrument change with frequency

Large bandwidth => Better imaging sensitivity $\sigma_{cont} = \frac{\sigma_{chan}}{\sqrt{N_{chan}}}$

- Angular-resolution increases at higher frequencies
- Sensitivity to large scales decreases at higher frequencies
- Wideband UV-coverage has fewer gaps => lower PSF sidelobe levels

1.0 GHz

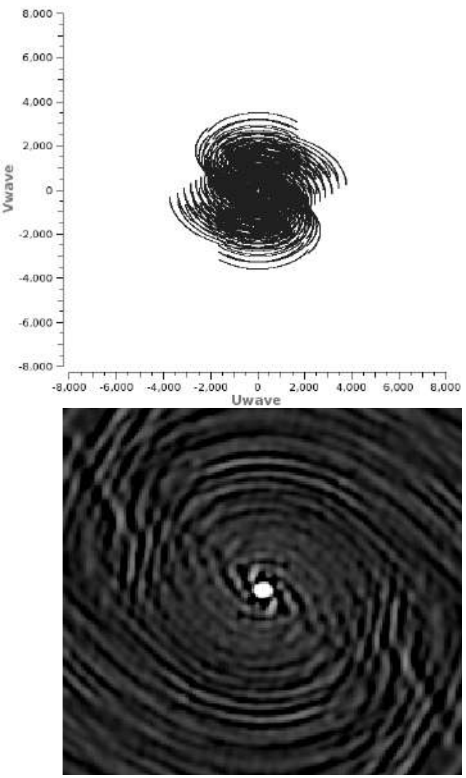

1.5 GHz

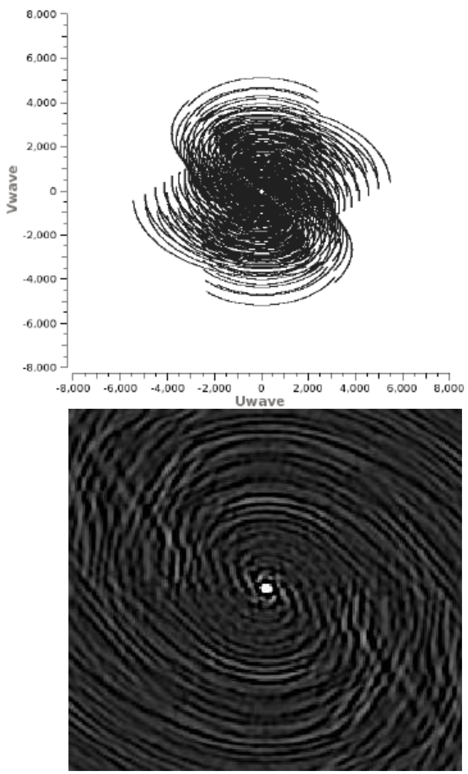

2.0 GHz

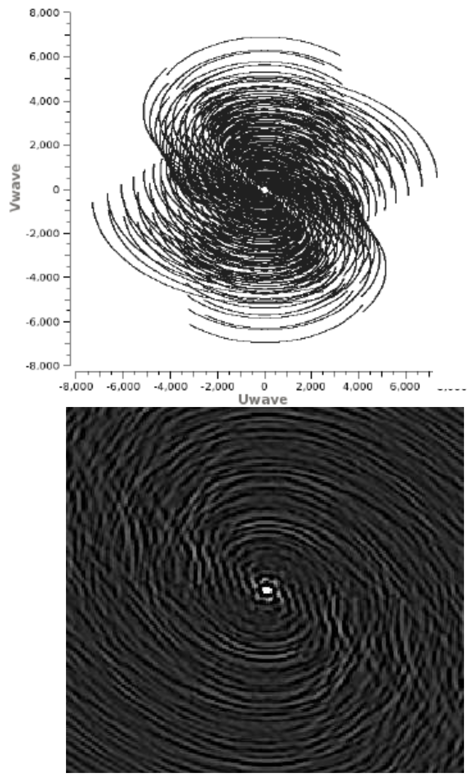

1.0 - 2.0 GHz

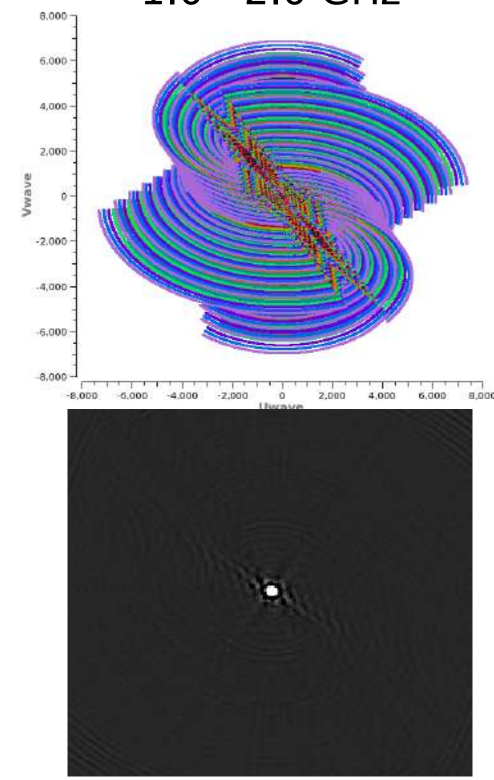

$$I_{wb}^{obs} = \sum_{\nu} \left[I_{\nu}^{sky} * PSF_{\nu} \right]$$

Observed image : $I_{\nu}^{obs} = I_{\nu}^{sky} * PSF_{\nu}$

Bandwidth smearing (over-averaging in frequency)

Excessive channel averaging of visibilities will cause radial smearing

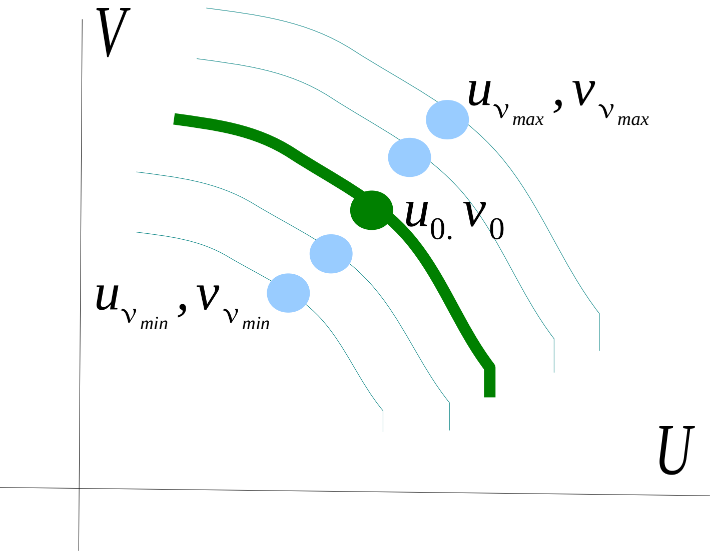

Suppose the entire receiver bandwidth was measured in one channel ν_0

$V(u_\nu)$ is mistakenly mapped to $\frac{\nu_0}{\nu} u_\nu$

Similarity theorem of Fourier-transforms :

Radial shift in source position with frequency.
=> Radial smearing of the sky brightness

2 MHz 200 MHz 1.0 GHz

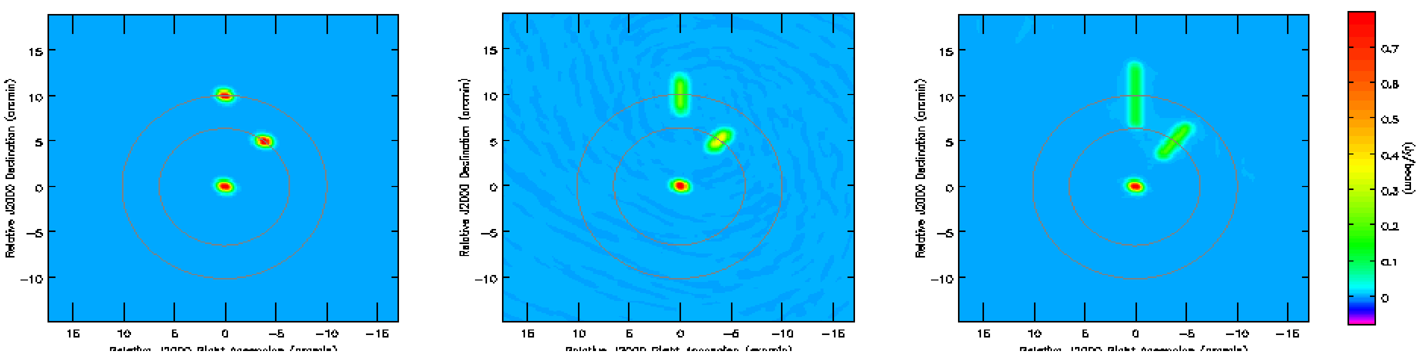

Bandwidth smearing limit for HPBW field-of-view :

$$\delta\nu < \frac{\nu_0 D}{b_{max}}$$

Bandwidth Smearing limits at L-Band (1.4 GHz),
33 MHz (VLA D-config), 10 MHz (VLA C-config),
3 MHz (VLA B-config), 1 MHz (VLA A-config)

Two wide-band imaging techniques : Cube / MFS

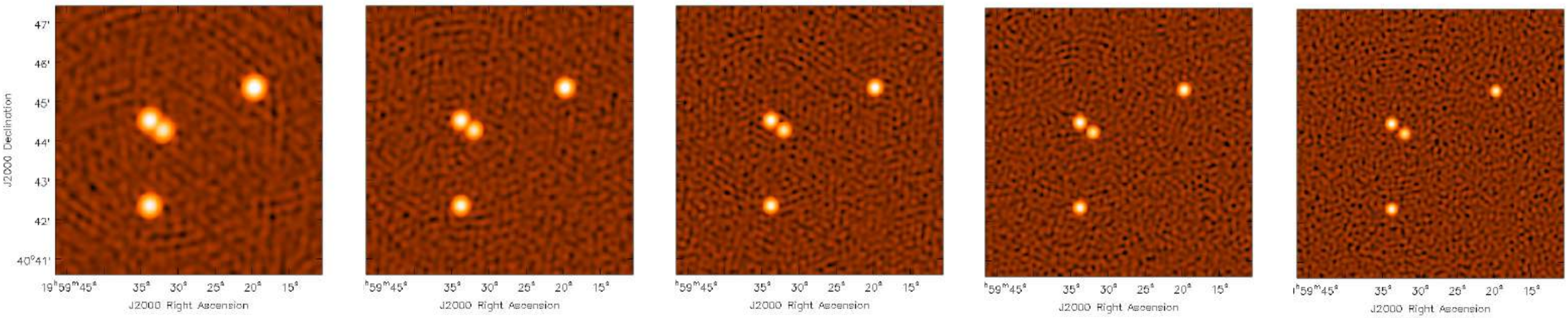

Cube Imaging :

(1) Reconstruct each chan/spw separately
(2) Smooth to the lowest available resolution
(3) Combine to calculate continuum and spectra

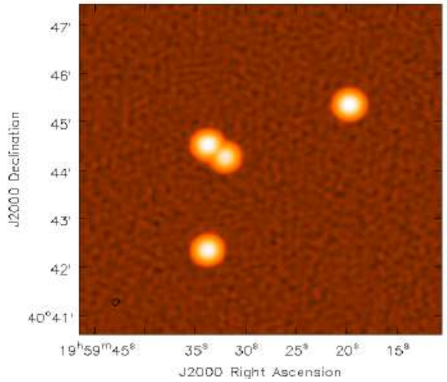

Multi-Frequency-Synthesis (MFS) :

Combine data from all frequencies onto
a single grid and do a joint reconstruction
(assuming flat sky spectra)

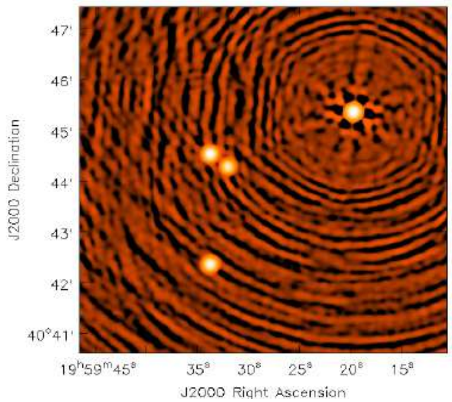

MFS with a wideband sky model (Multi-Term MFS)

Solve for spectral Taylor polynomial coefficients $$I_\nu^{sky} = \sum_t I_t^m \left(\frac{\nu - \nu_0}{\nu_0} \right)^t$$

(Multi-term linear least squares)

Interpret coefficients as a power-law (spectral index and curvature)

$$I_\nu = I_{\nu_0} \left(\frac{\nu}{\nu_0} \right)^{\alpha + \beta \log(\nu/\nu_0)} \longleftrightarrow \quad I_0^m = I_{\nu_0} \qquad I_1^m = I_{\nu_0} \alpha \qquad I_2^m = I_{\nu_0} \left(\frac{\alpha(\alpha-1)}{2} + \beta \right)$$

Rau &Cornwell, 2011
Sault &Wieringa, 1994

Nterms=1
(ignore spectra)

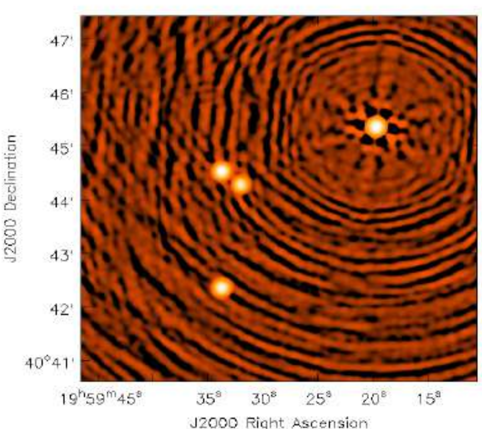

NTerms>1
(Model the spectrum during the reconstruction)

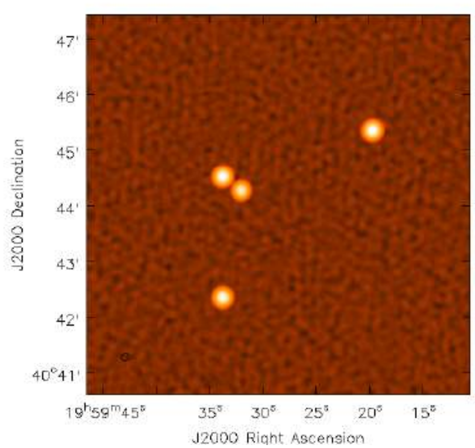

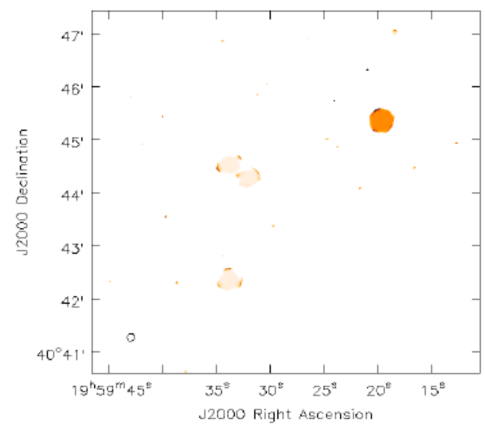

Dynamic-range (MT-MFS, 1-2 GHz 3C286, Nt=1,2,3,4)

Strong sources => More terms in spectral model => High dynamic range

NTERMS = 1

Rms :
9 mJy -- 1 mJy

DR :
1600 - 13000

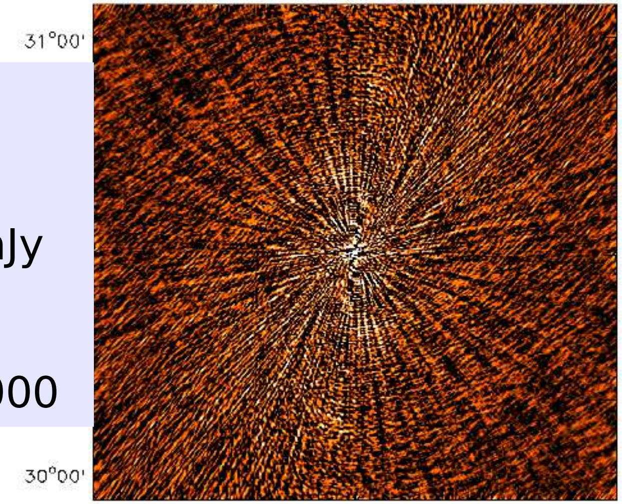

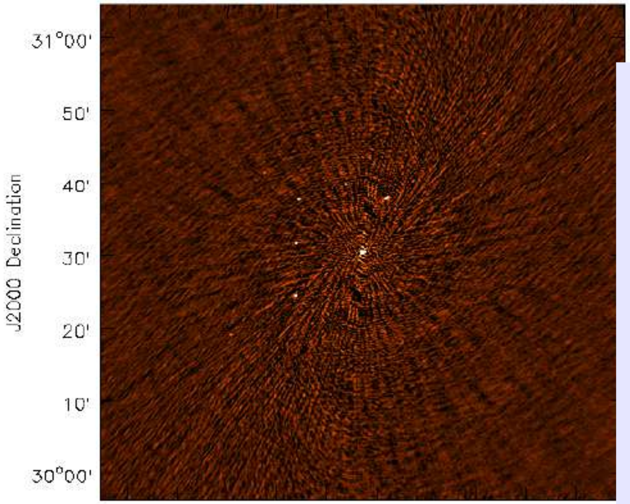

NTERMS = 2

Rms :
1 mJy -- 0.2 mJy

DR :
10,000 - 17,000

NTERMS = 3

Rms :
0.2 mJy -- 85 uJy

DR :
65,000 - 170,000

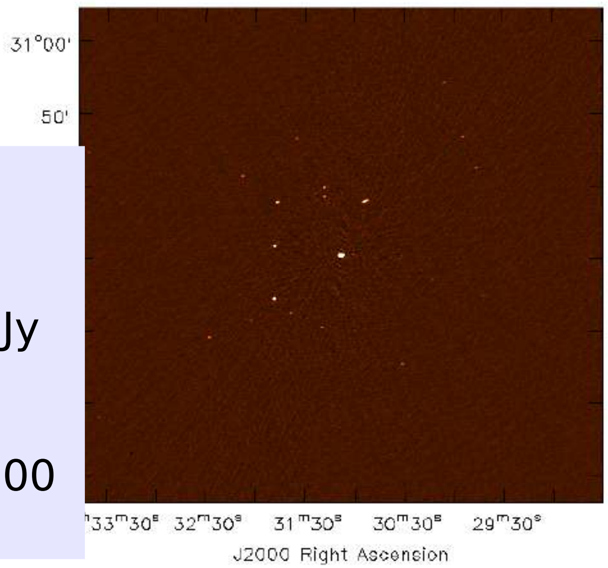

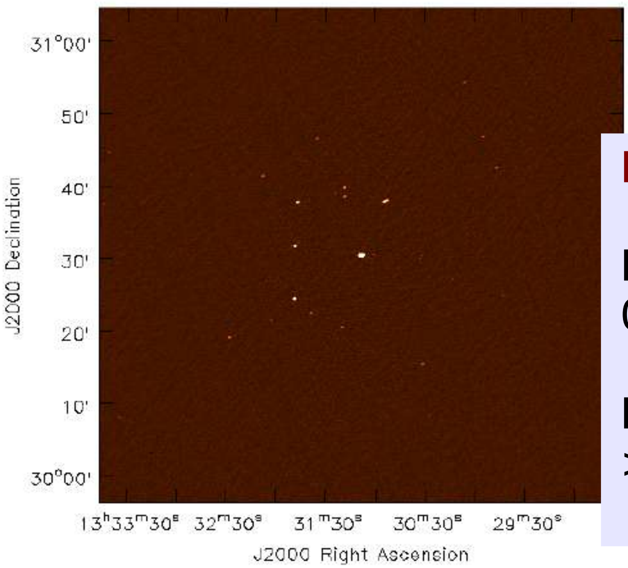

NTERMS = 4

Rms
0.14 mJy -- 80 uJy

DR :
>110,000
- 180,000

.... needs well-calibrated data

Wideband Imaging Quality - Comparison

Cube

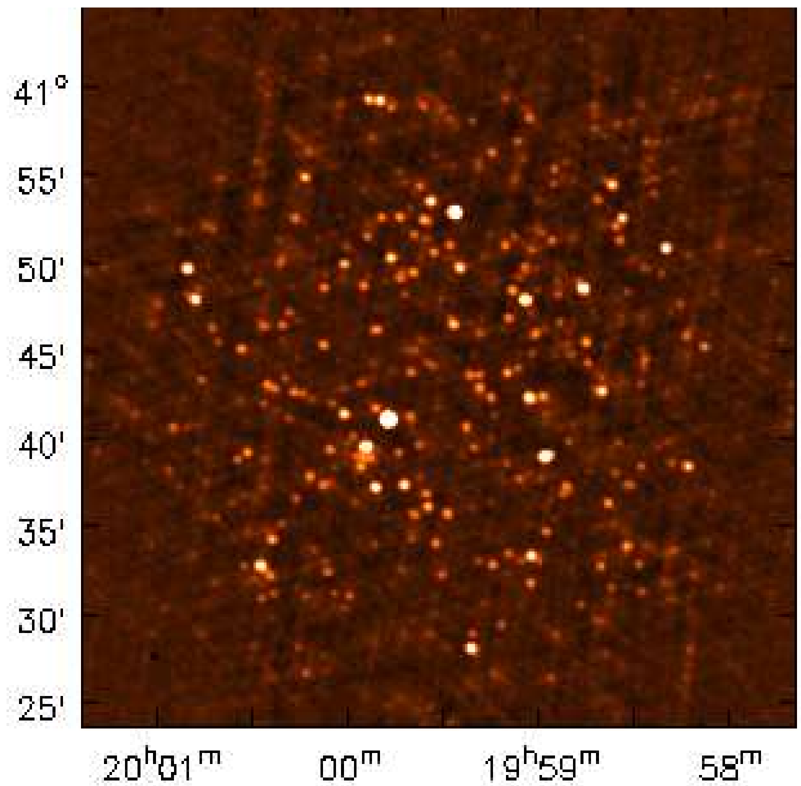

- Low angular resolution
- Weakest sources are not deconvolved enough
- Crowded field may suffer from 'Clean bias' due to PSF sidelobes and require careful masking
+ Independent of spectral model

(MT) MFS

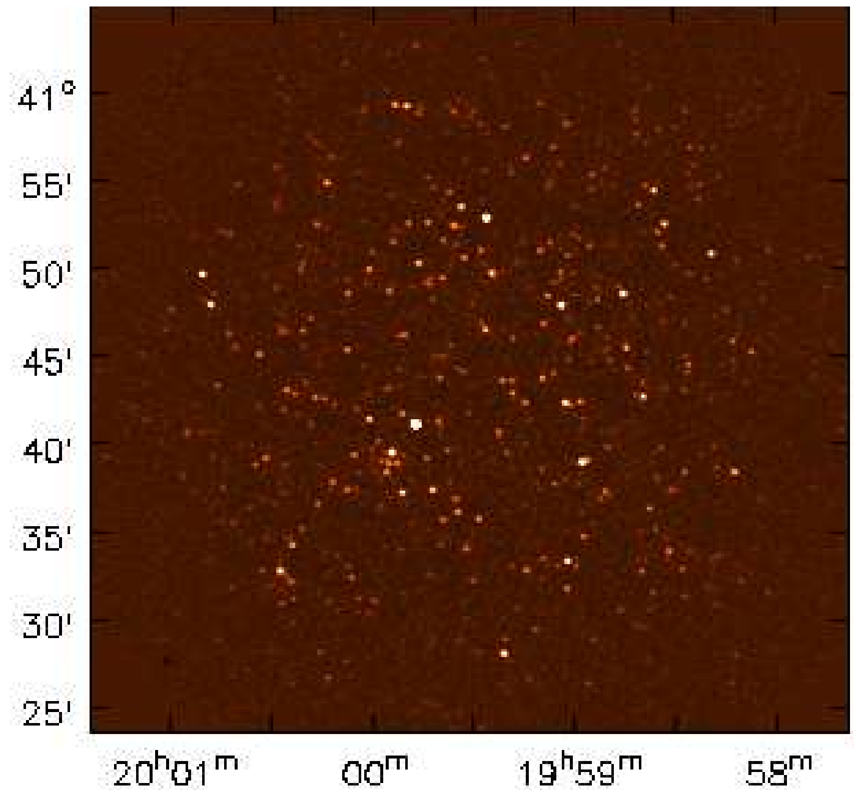

+ High angular resolution
+ Imaging at continuum sensitivity
+ Better PSF and imaging fidelity can eliminate 'Clean bias' and the need for masks in crowded fields
- Depends on how appropriate the spectral model is

Spectral Index Accuracy (for low SNR)

Accuracy of the spectral-fit increases with larger bandwidth-ratio

1 – 2 GHz, 4 hr

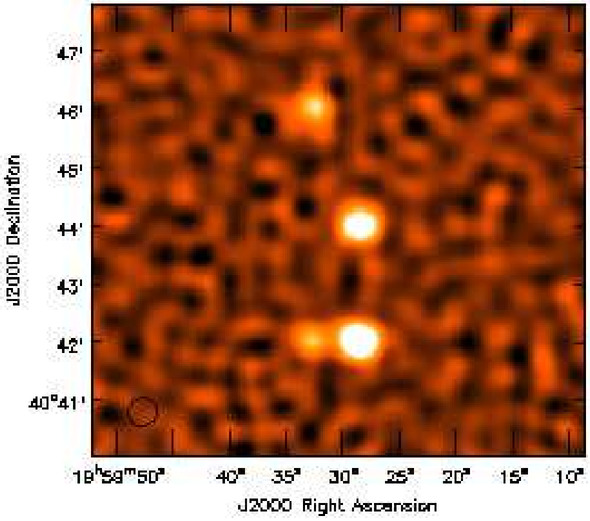

4 - 8 GHz , 4 hr

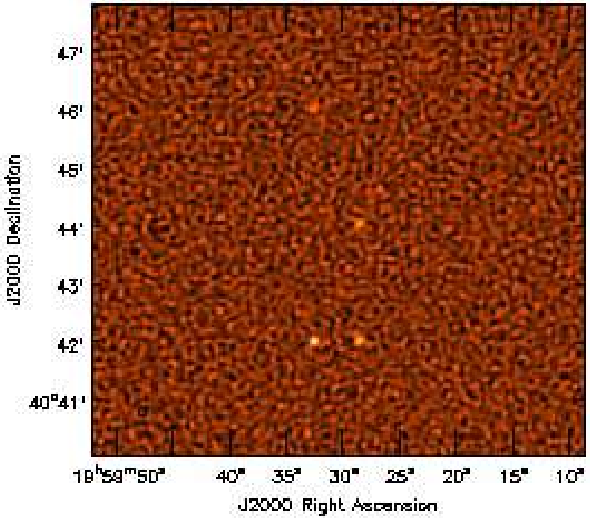

1 – 2 GHz, 4 - 8 GHz, 2 hrs each

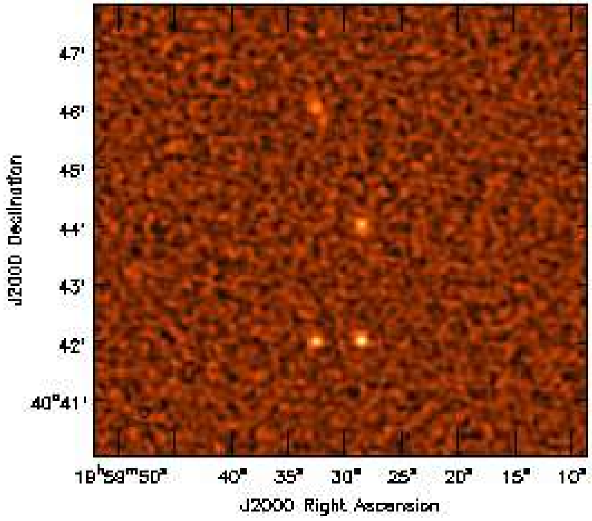

RMS
5 uJy/bm

Source	Peak Flux	SNR	L alpha	C alpha	LC alpha	True
Bottom right	100 uJy	20	-0.89	-1.18	-0.75	-0.7
Bottom left	100 uJy	20	+0.11	+0.06	+0.34	+0.3
Mid	75 uJy	15	-0.86	-1.48	-0.75	-0.7
Top	50 uJy	10	-1.1	0	-0.82	-0.7

To trust spectral-index values, need SNR > 50 (within one band – 2:1)
For SNR < 50 need larger bandwidth-ratio.

Angular resolution of MFS (wideband) images

Can model the intensity and spectrum at the angular resolution of the highest frequency channel (high SNR)

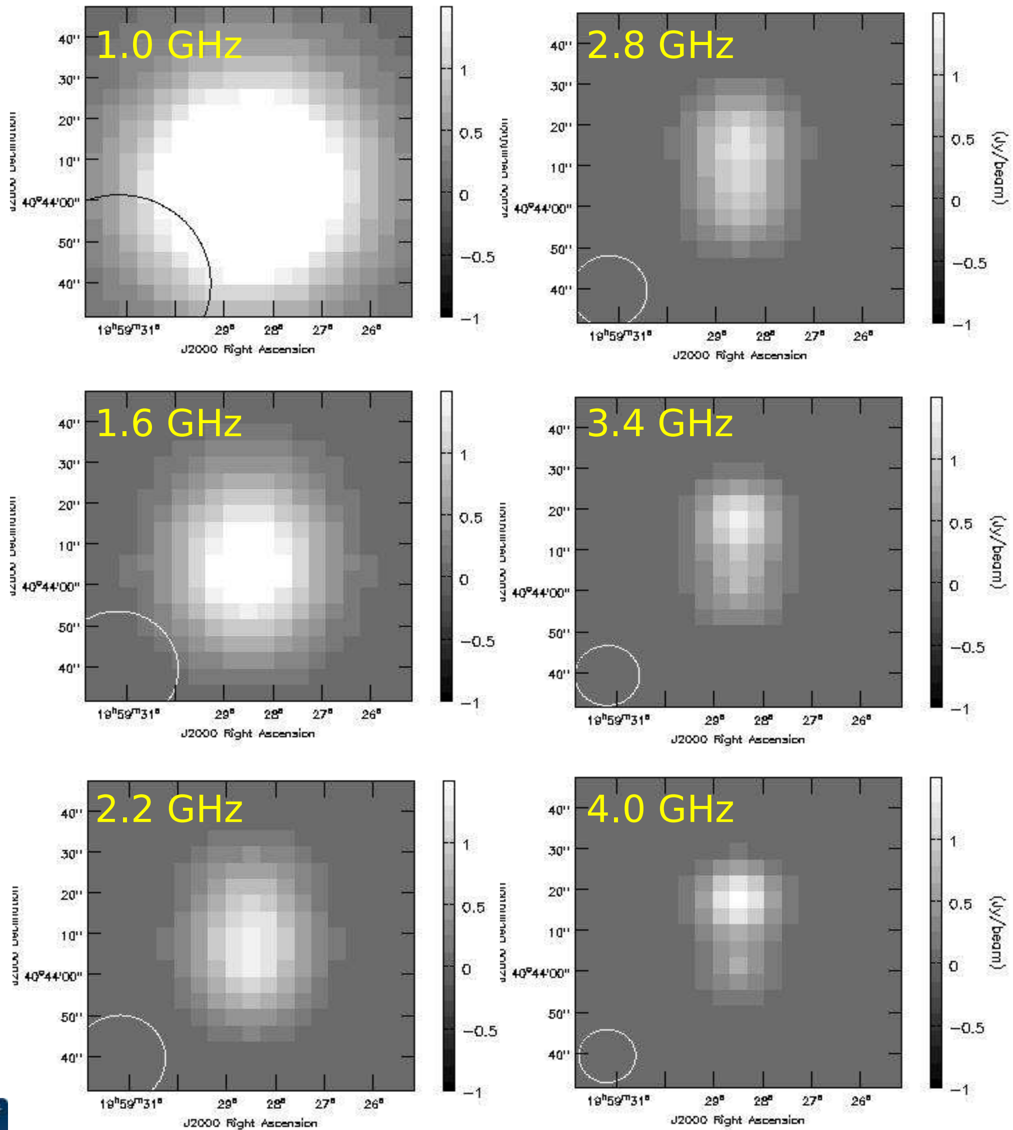

Restored Intensity image

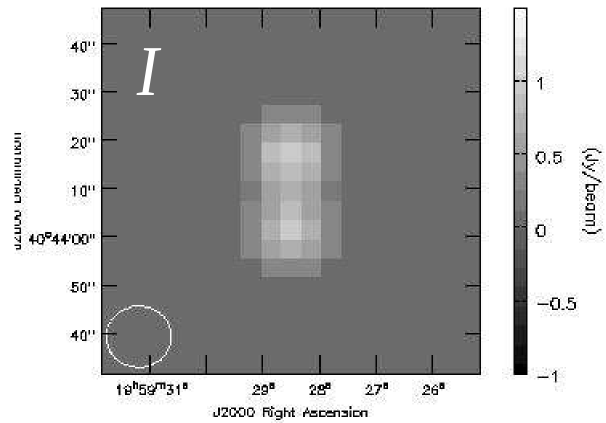

Spectral Index map

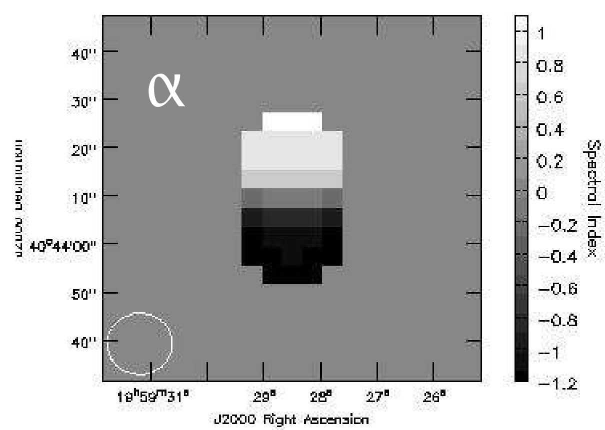

Wideband (MTMFS) imaging of extended-emission

A good multi-scale model gives better spectral index and curvature maps

Intensity Image

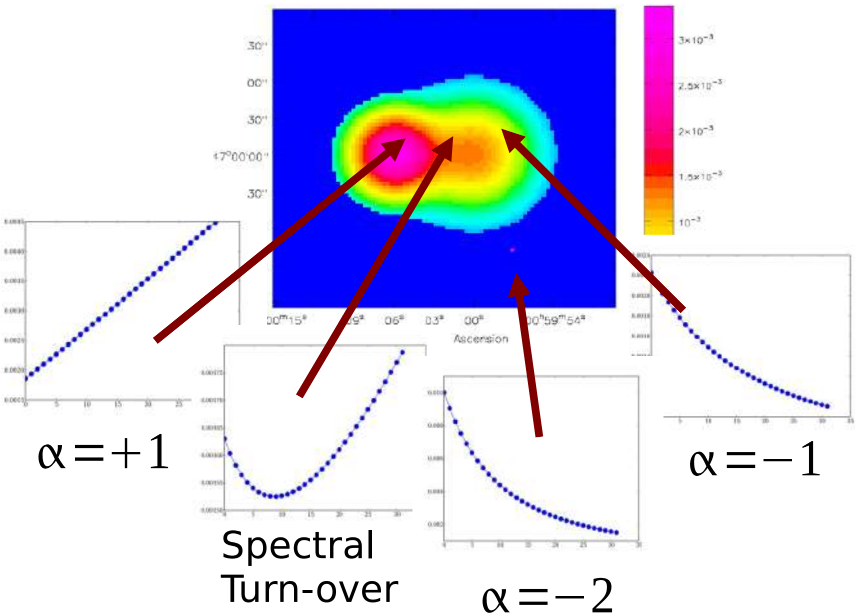

Average Spectral Index

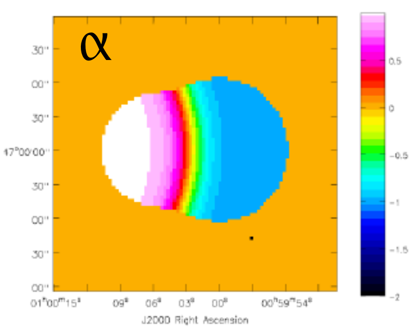

Gradient in Spectral Index

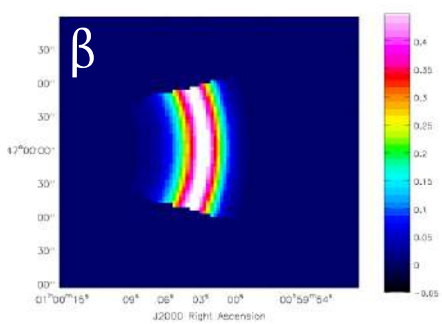

MT-MFS

multi-scale **point-source**

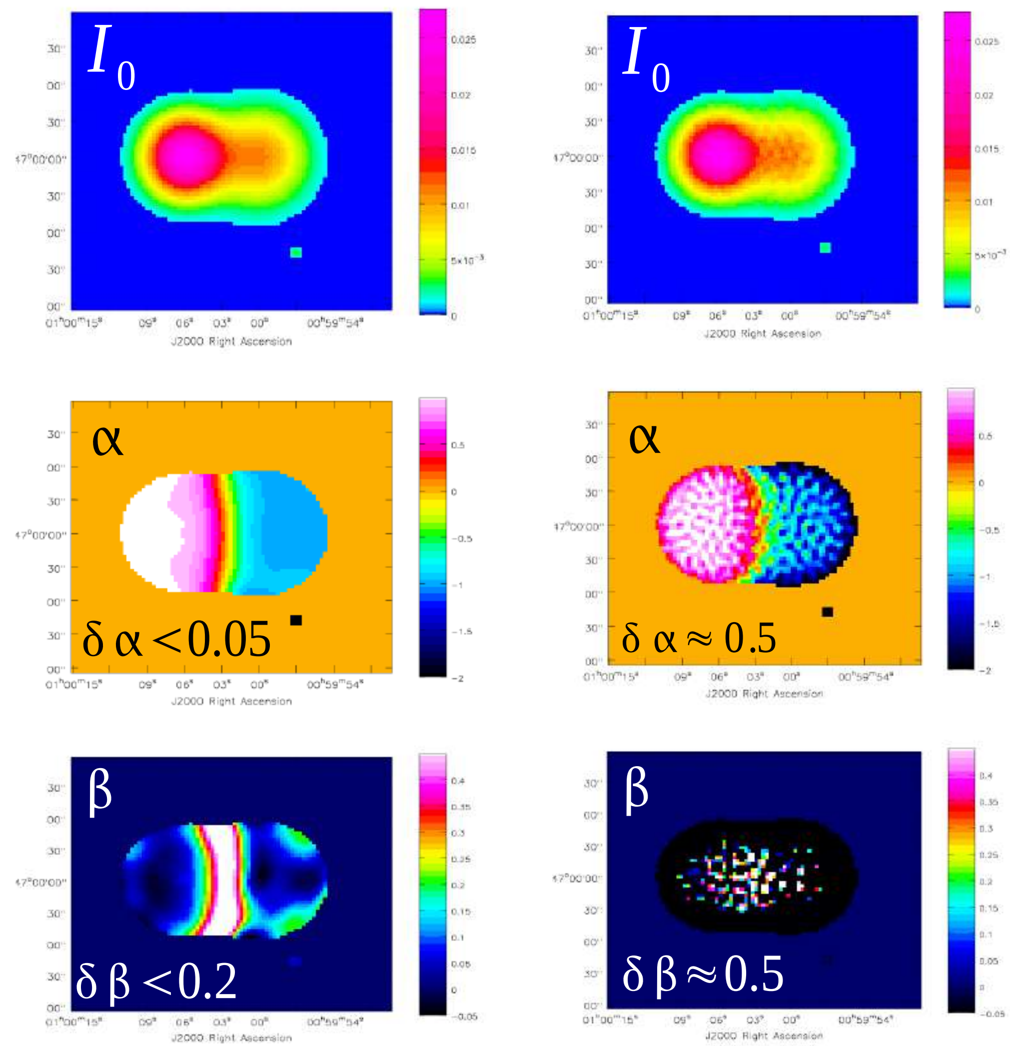

=> Spectral-index error is dominated by 'division between noisy images'

Supernova Remnants at L and C Band [Bhatnagar et al, 2011]

Examples of typical accuracy of spectral index maps (extended emission)

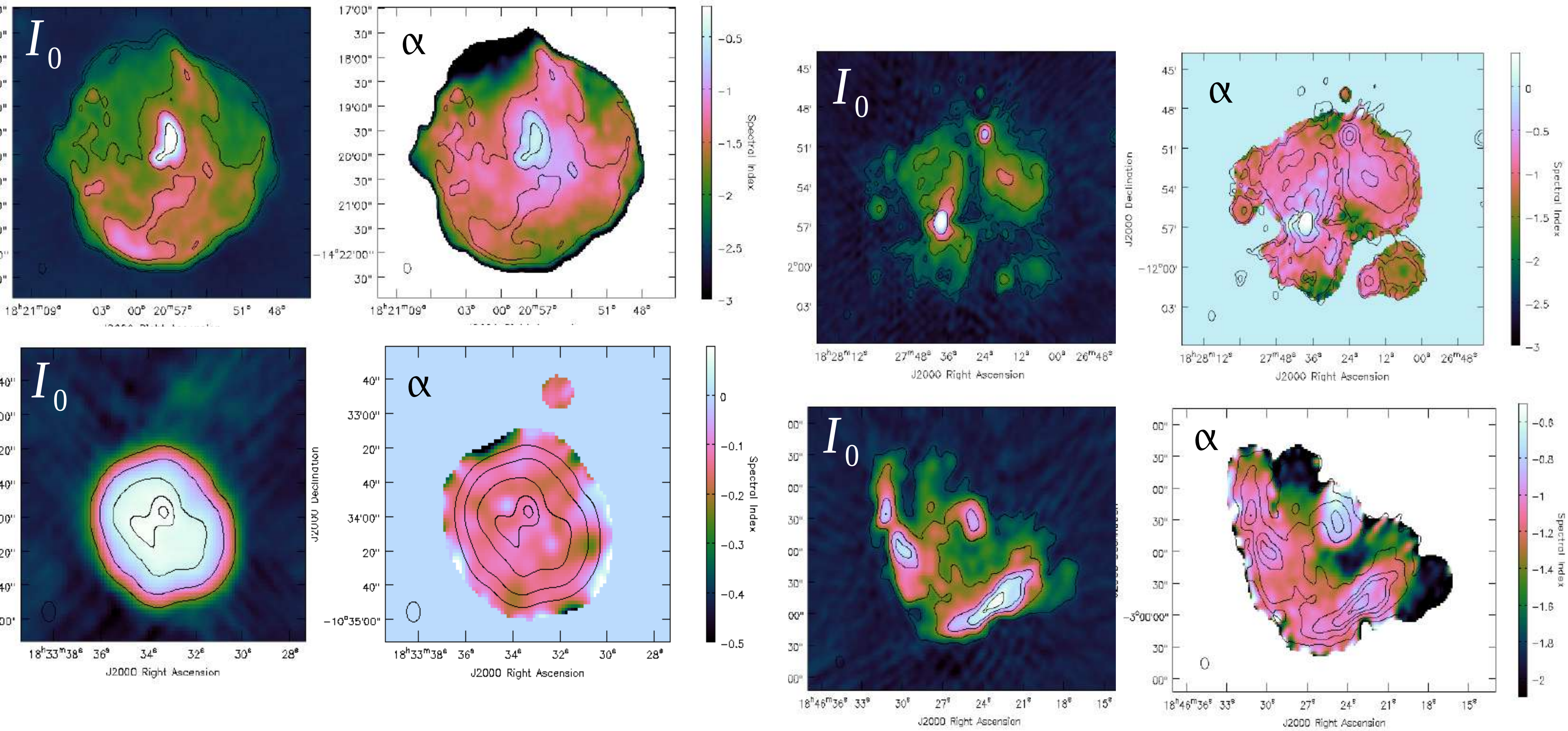

These examples used nterms=2, and about 5 scales.

=> Within 1-2 Ghz and 4-8 GHz, spectral-index error is < 0.2 for SNR>100.
=> Dynamic-range limit of few x 1000 ---> residuals are artifact-dominated

Example : Abell 2256 *[Owen et al, 2014]*

Example of high-fidelity wideband imaging (and, a pretty picture !)

Intensity

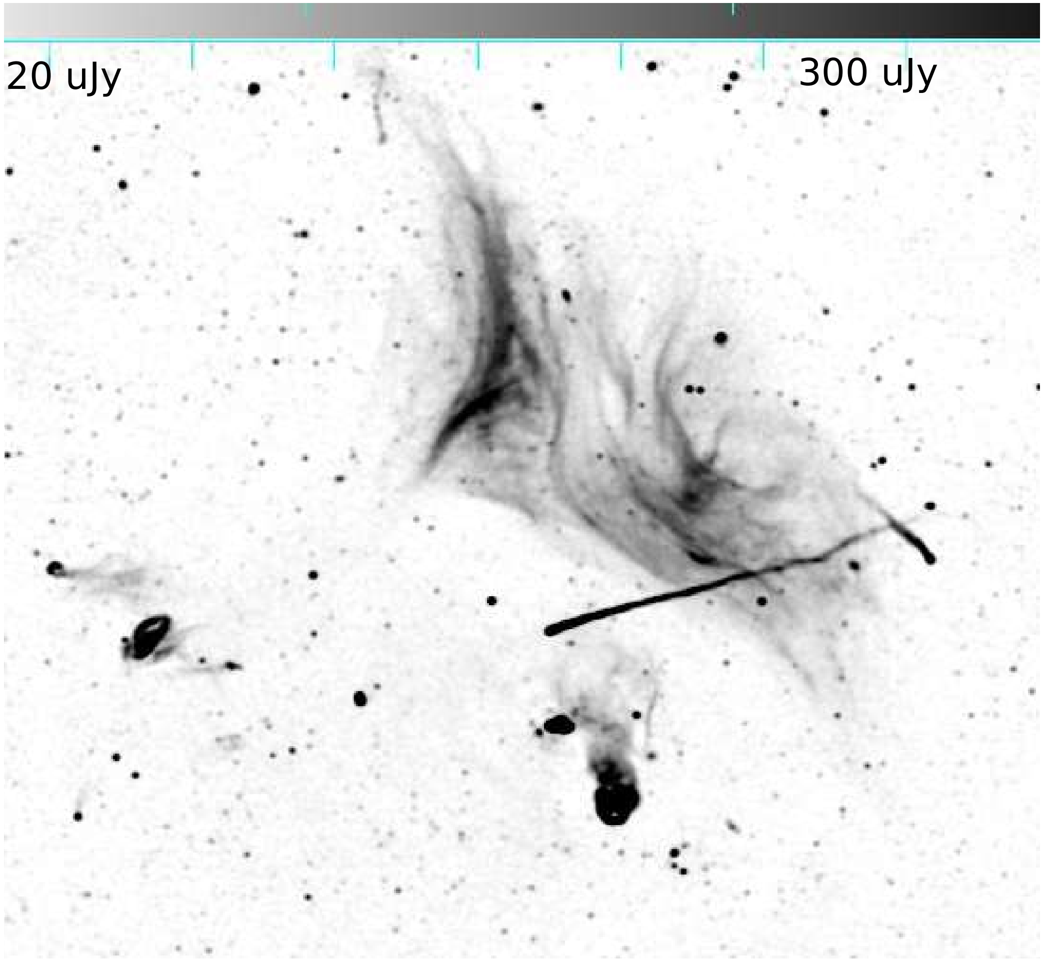

Intensity weighted Spectral Index

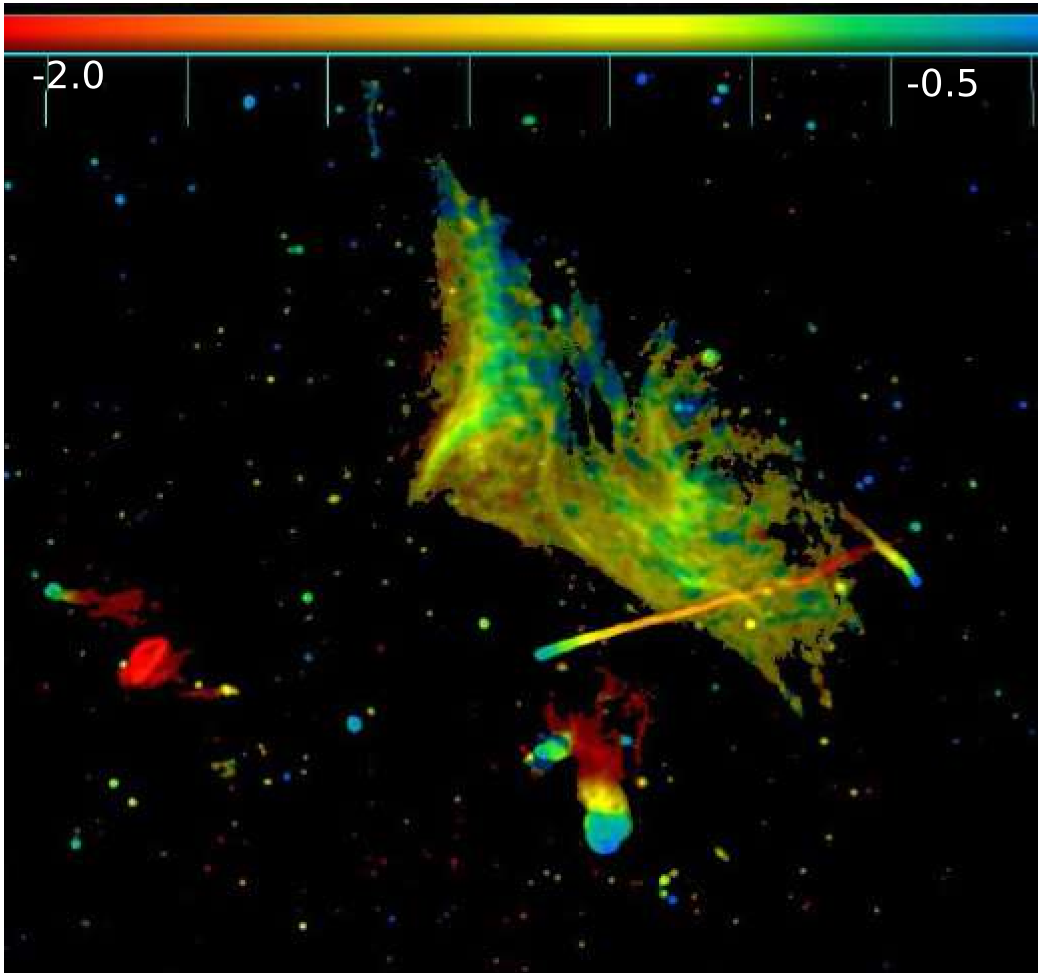

VLA A,B,C,D at L-Band (1-2 GHz), VLA A at S&C bands(2-4, 4-6, 6-8 GHz)

Calibration and Auto-flagging in AIPS. Intensity/Spectral index Imaging in CASA.

Wide Band Imaging

(sky and instrument change with frequency)

Wide Field Imaging

(non-coplanar baselines and the W-term)

Full Beam Imaging

(antenna primary beams)

Wide-Field Imaging – W-term

Geometrical effects => 2D Fourier transform relation does not hold

$$V^{obs}(u,v) = S(u,v) \iiint I(l,m)\, e^{2\pi i (ul + vm + w(n-1))}\, dl\, dm\, dn$$

- **w** and **n** increase with distance from the image phase center
- **w** increases with baseline length and observing frequency
- Array is not instananeously coplanar

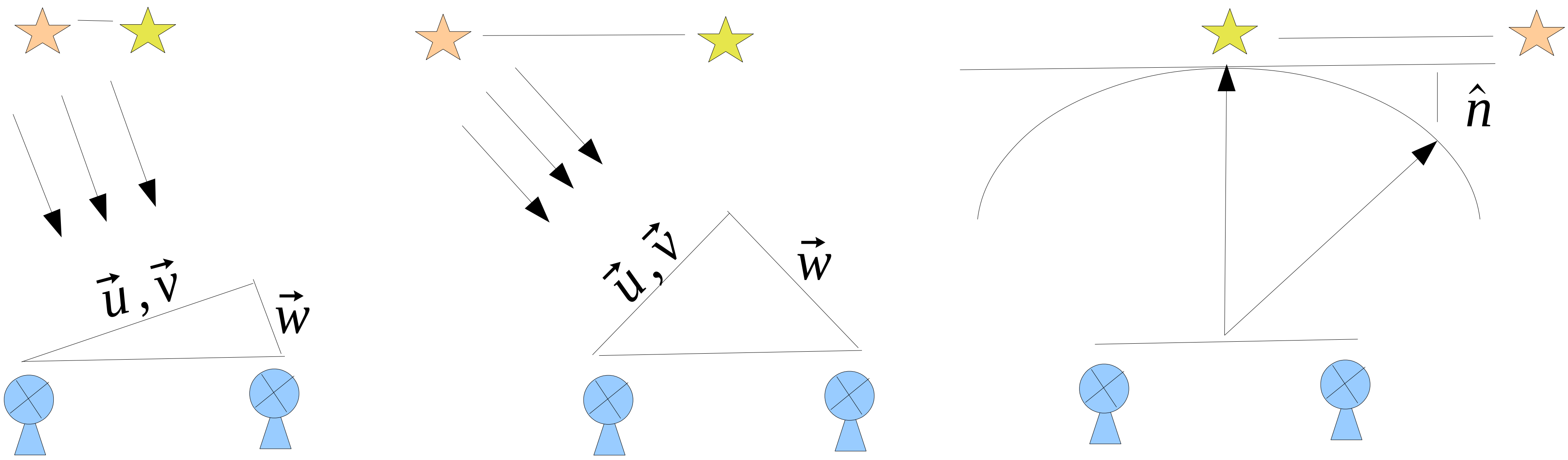

Example : For the VLA, the W-term becomes significant at a radius of
- 1 deg for D-config, L-band (PB : 30arcmin)
- 2 arcmin for A-config, L-band (PB : 30 arcmin) [Ref. R.Perley's talks]

W-term : Effect on images + Solutions

Time-dependent position shift => Smearing into arc-like patterns

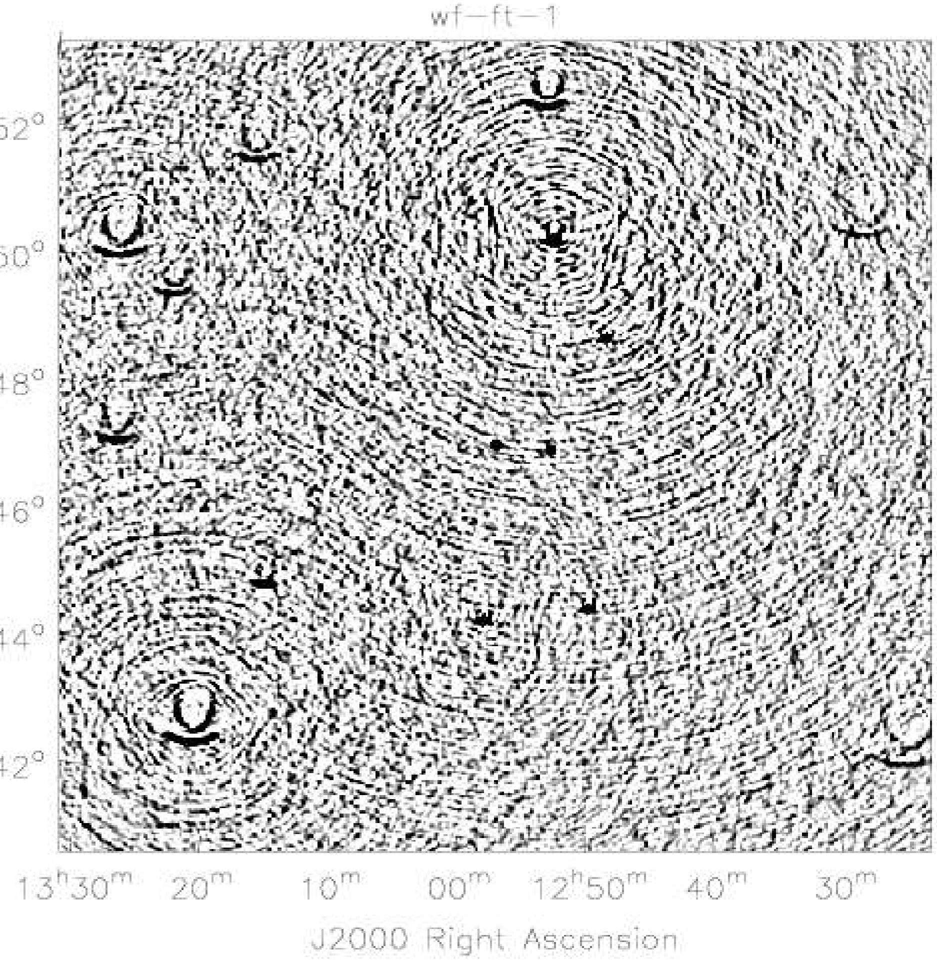

Arcs or shifts for sources away from phase center

W-term is a phase error. Sources move systematically in the image
(Weak sources can disappear)

There are four ways to handle this
(Ref. R.Perley's talk)

- 3D imaging : Image the curved sky
- W-stacking : Re-grid snapshot images to single coordinate sys.
- Faceting : Sub-images with own phase reference centers
- W-Projection : Undo it during gridding

W-term : Algorithms : Faceting

- Approximate the celestial sphere by a set of tangent planes (facets) such that 2D geometry is valid per facet

- Image each facet with its own phase reference center and re-project to the tangent plane

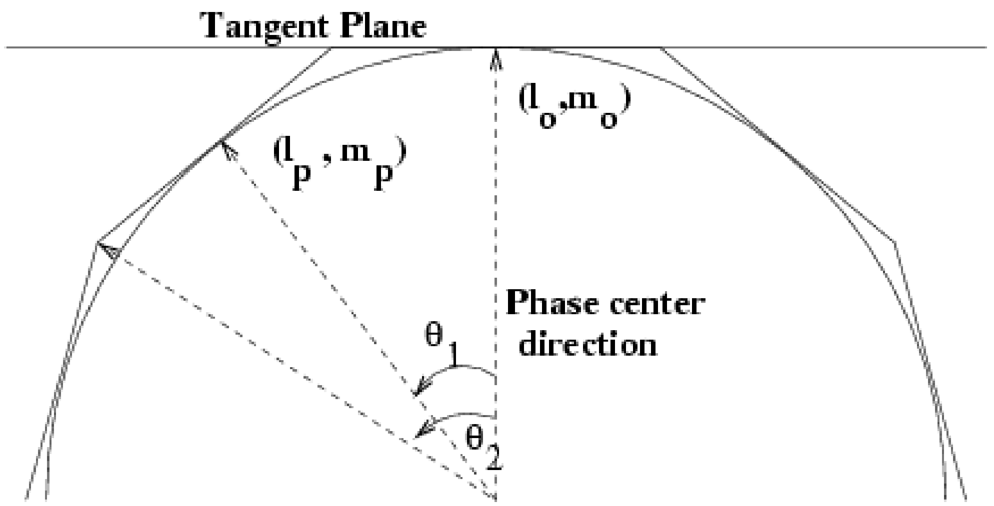

Variants:

Deconvolve facets separately before re-projecting and stitching

(or)

Image all facets onto the same tangent plane grid and perform a joint deconvolution.

Number of facets : $N_{Poly} = \theta_f^2 \frac{B_{max}}{\lambda} max = \frac{B_{max} \lambda_{max}}{[N_{lobes} D]^2}$ $\quad D \equiv Antenna\ diameter;\ \ \theta_f = Antenna\ FoV$

W-term : Algorithms : W-Projection

For ideal 2D imaging we need to measure $E_1^{'}$. Instead we measure E_1

$E_1^{'}$ and E_1 are related by a Fresnel diffraction/propagation kernel.

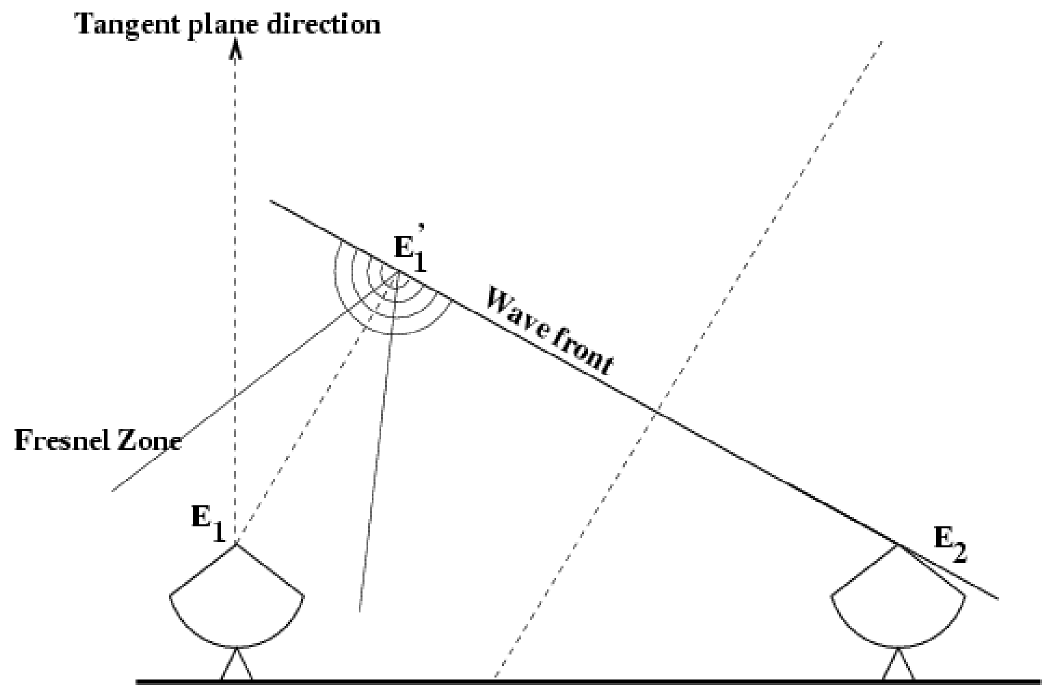

$$G(u,v,w)=FT\left[e^{2\pi\iota w\sqrt{1-l^2-m^2}}\right]$$

$$V^o(u,v,w)=V(u,v,w=0)*G(u,v,w)$$

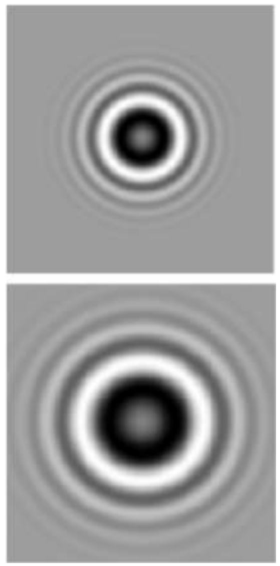

Convolution in uv-domain

=> Correct it by another convolution with the inverse/conjugate kernel (during the gridding step)

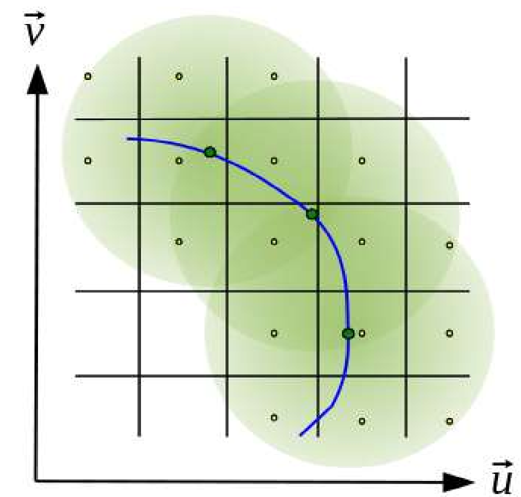

=> Use different kernels for different W values (appropriately quantized)

W-term : Example

Cornwell et al, 2008

2D Imaging

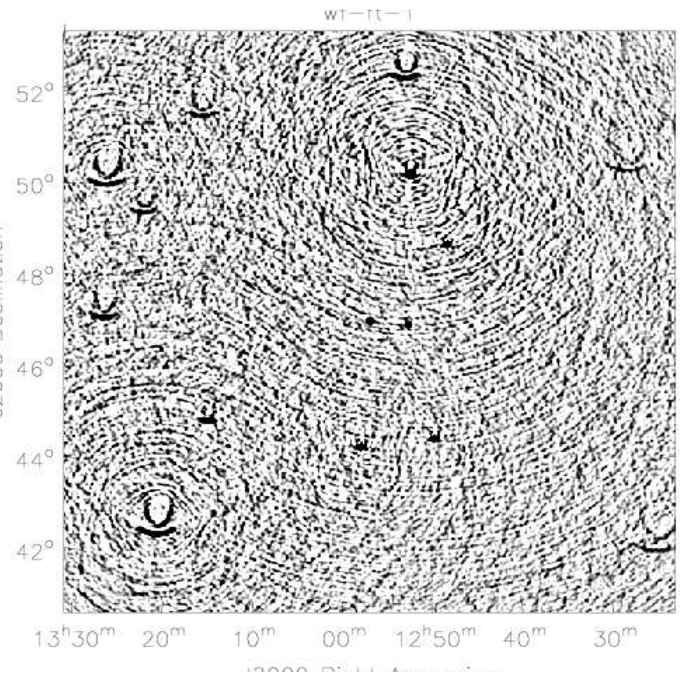

Facet Imaging

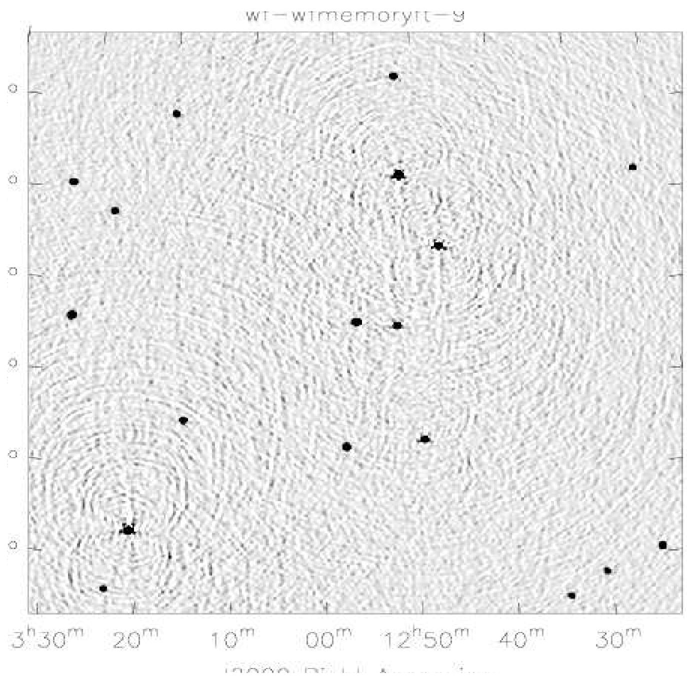

W-Projection

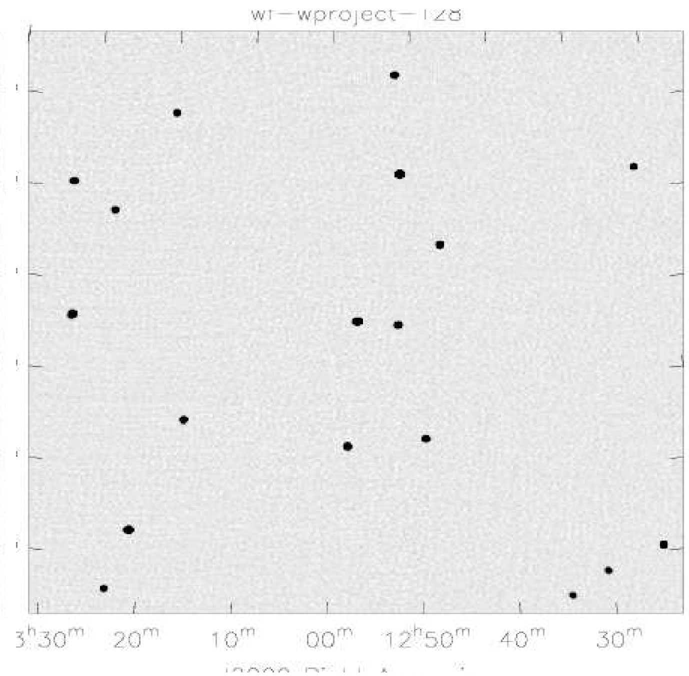

In general, W-Projection is more accurate and faster.

But, for very wide fields of view (such as those offered by dipole arrays), W-Projection kernels may become too large

=> Use a combination of faceting and W-Projection
=> Or, use W-Stacking

W-term : W-Projection example (74MHz VLA)

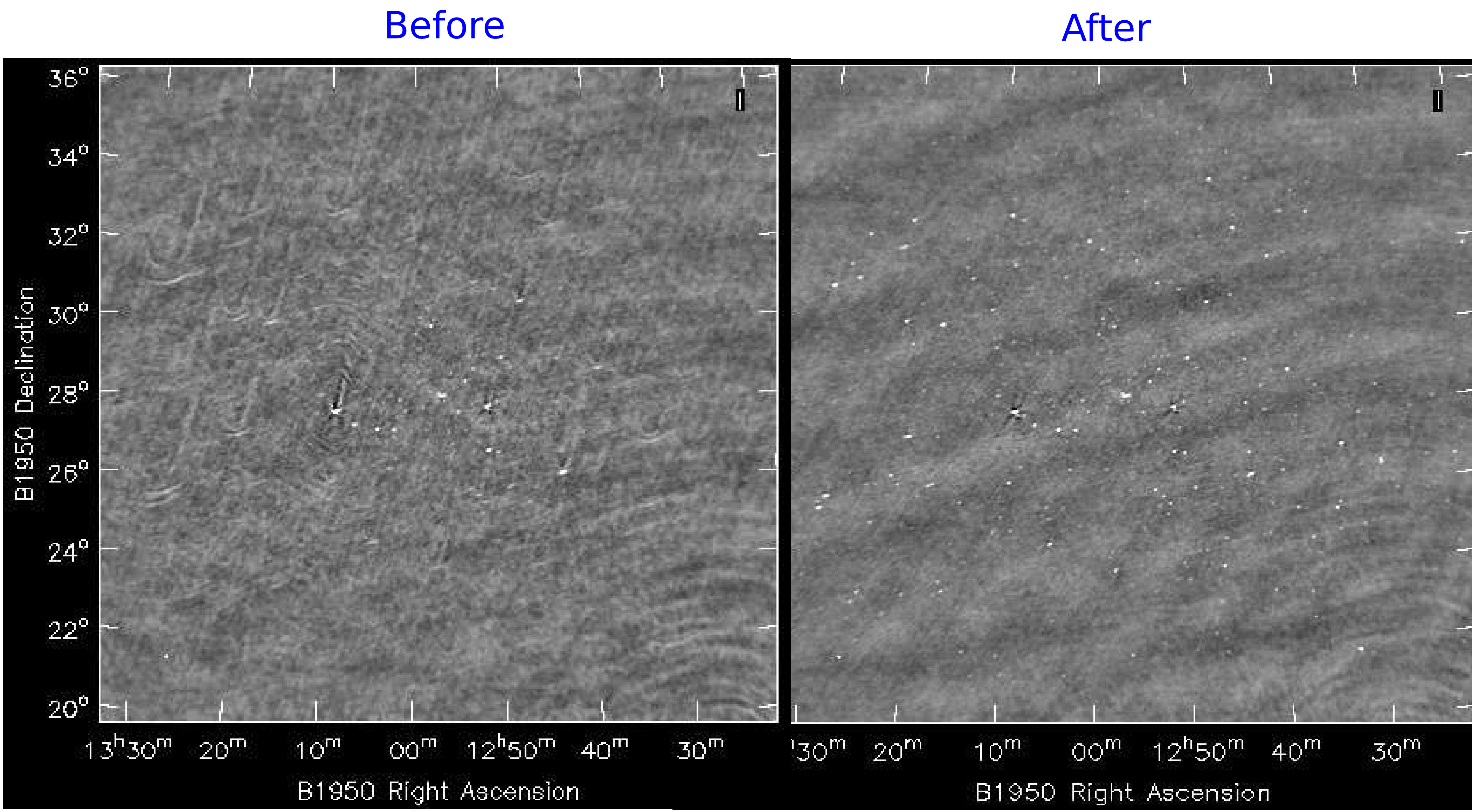

Images from K.Golap

Wide Band Imaging

(sky and instrument change with frequency)

Wide Field Imaging

(non-coplanar baselines and the W-term)

Full Beam Imaging

(antenna primary beams)

Wide-Field Imaging – Primary Beams

The Sky is multiplied by a PB, **before** being sampled by each baseline

$$I^{obs}(l,m)=\sum_{ij,t} I_{ij}^{PSF}(l,m,t) \ast \left[P_{ij}(l,m,t)\cdot I^{sky}(l,m)\right]$$

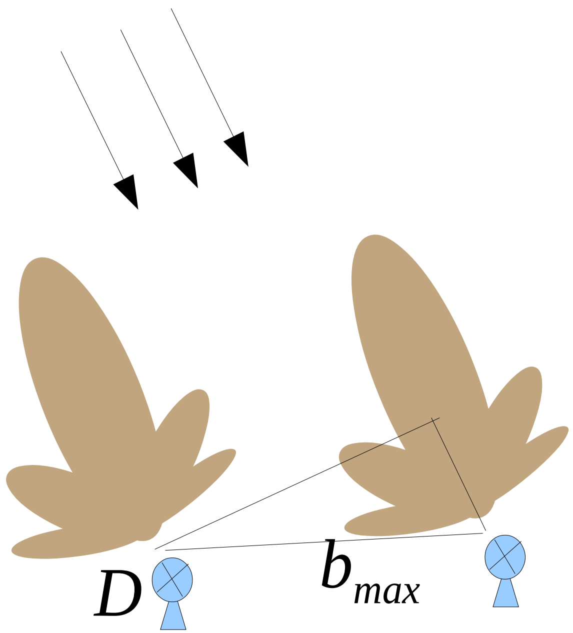

The antenna field of view :
D = antenna diameter

$$\lambda / D$$

Primary Beam
for baseline ij

P_{ij}

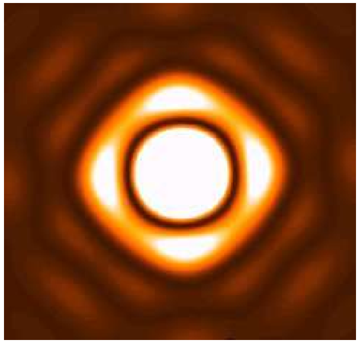

$$P_{ij} = V_i . V_j^{*} = FT\left[A_i \ast A_j^{*}\right] = FT\left[A_{ij}\right]$$

Aperture
Illumination
for antennas
i and j : A_i , A_j

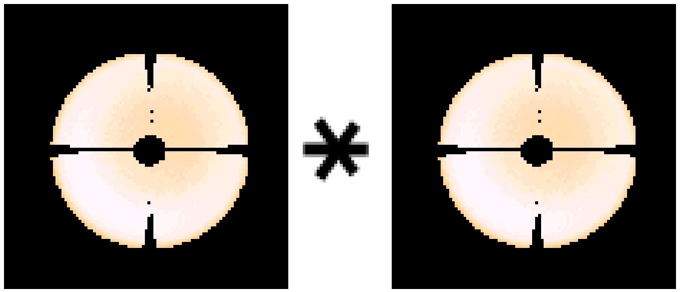

$A_{ij} =$ Baseline aperture Illumination

Primary Beam Correction – ‘pbcor’

Assume identical primary beams

$$I^{obs}(l,m) \approx I^{PSF}(l,m) * \left[P^{sky}(l,m) \cdot I^{sky}(l,m)\right]$$

=> Divide out an average primary beam model after deconvolution

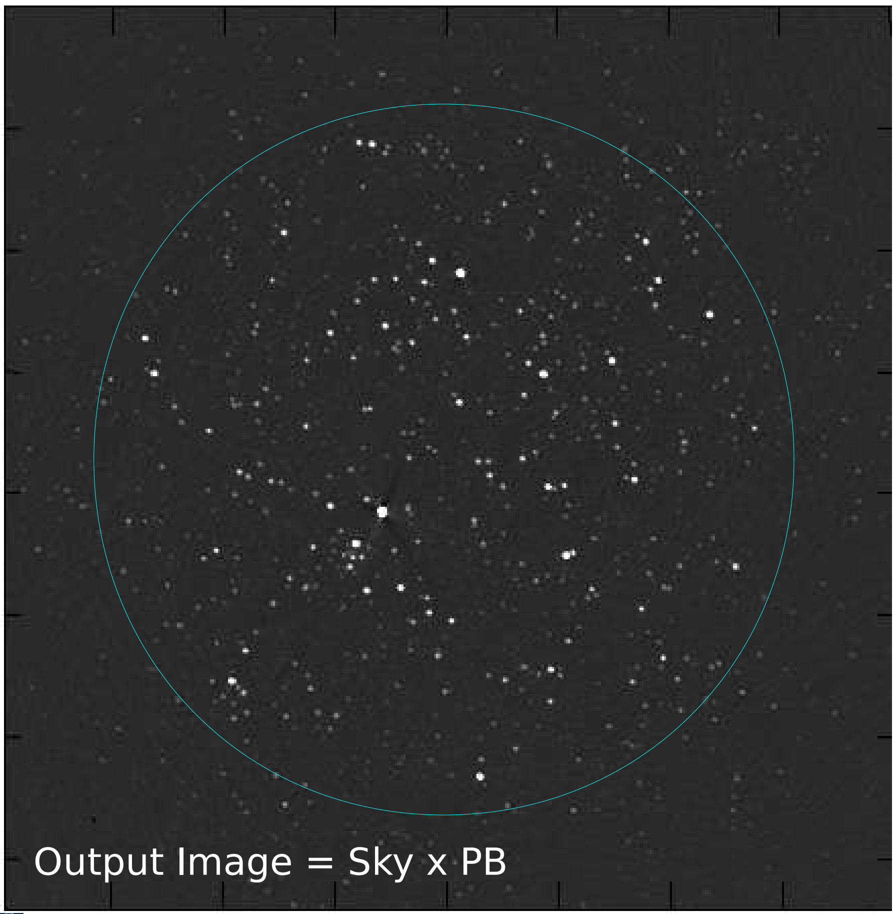

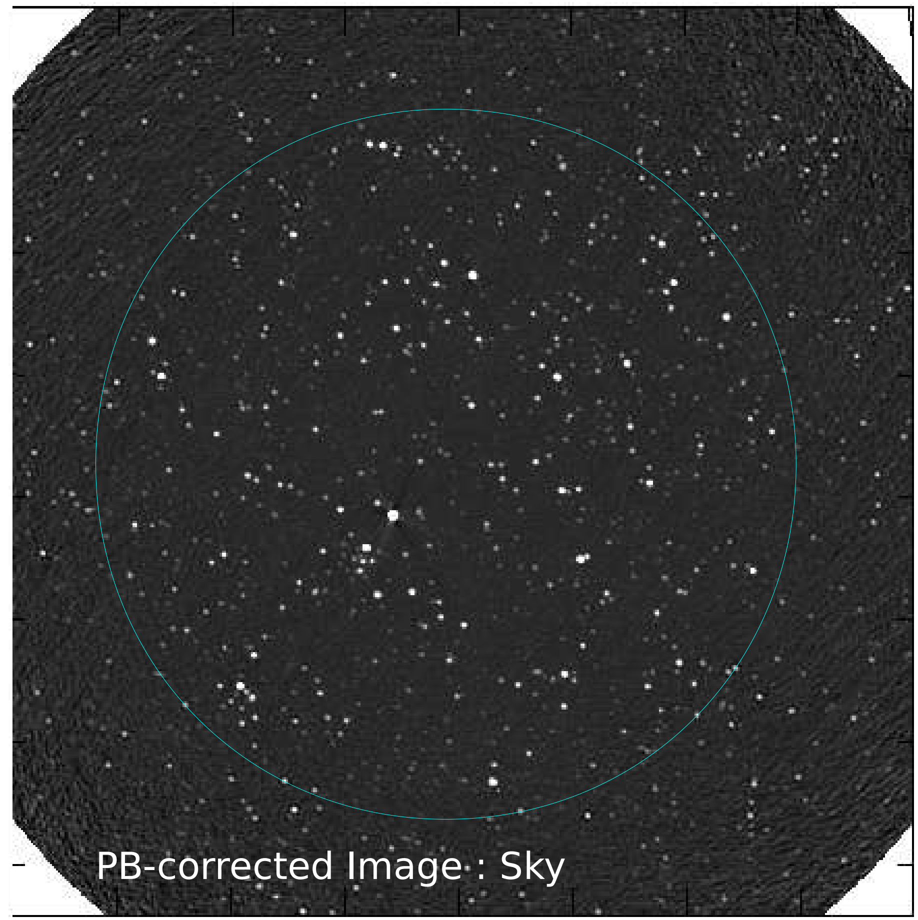

Primary beams vary within an observation

PB rotates with time, for alt-az mount antennas. (e.g. VLA)

PB varies from antenna to antenna within the array (e.g. ALMA)

PB shape changes with direction on the sky for aperture arrays (e.g. LWA)

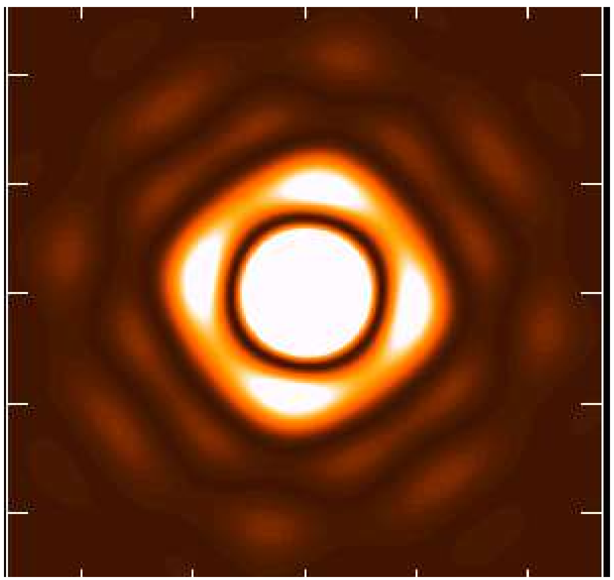

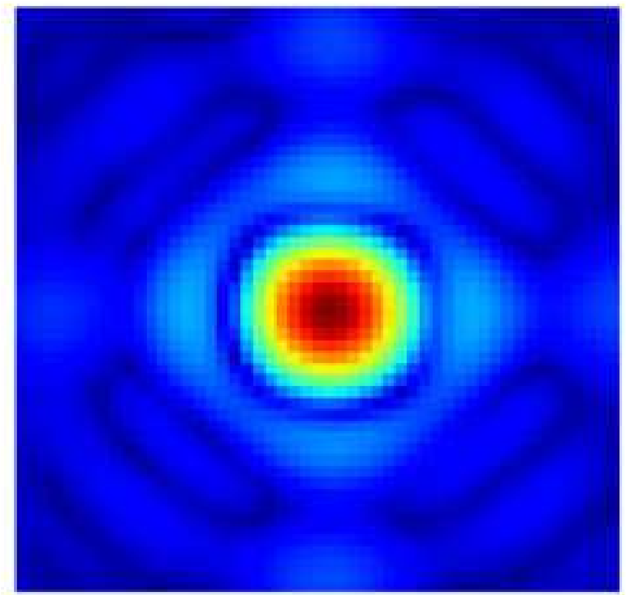

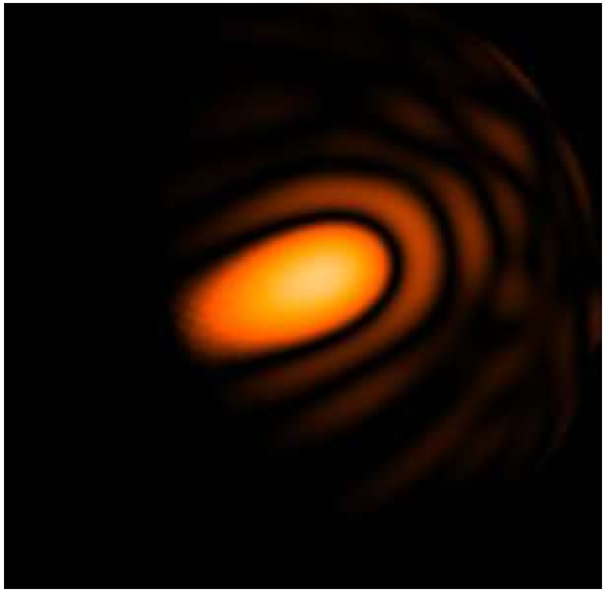

VLA has beam squint

Stokes V

(R – L)

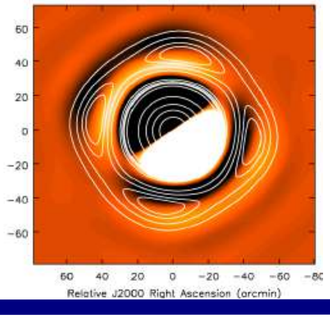

Typically for the ALMA and VLA, errors occur at the 10^4 dynamic range level if such primary beam variations are ignored. Beam squint and pointing offsets cause the dominant errors. For aperture arrays, the shape cannot be ignored.

Primary beams vary within an observation

PB rotates with time, for alt-az mount antennas. (e.g. VLA)

PB varies from antenna to antenna within the array (e.g. ALMA)

PB shape changes with direction on the sky for aperture arrays (e.g. LWA)

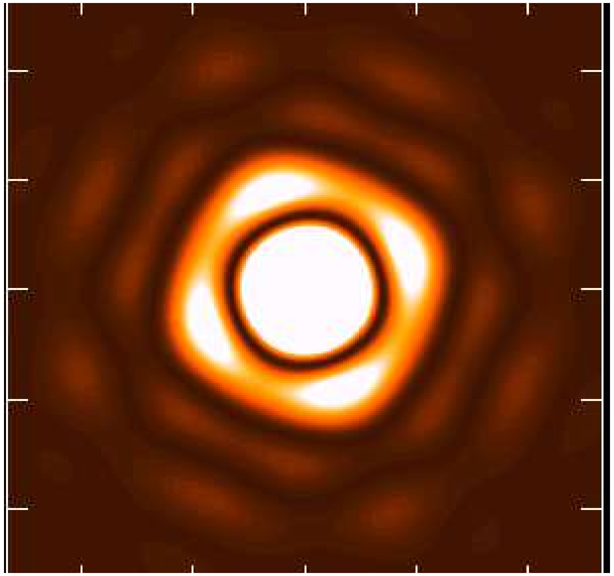

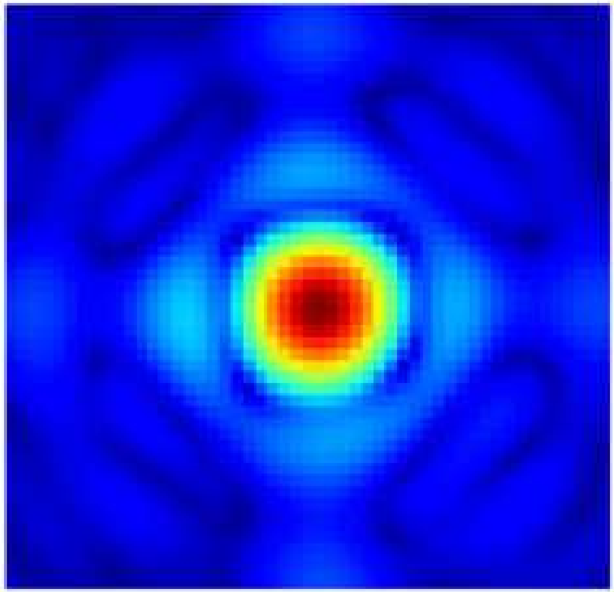

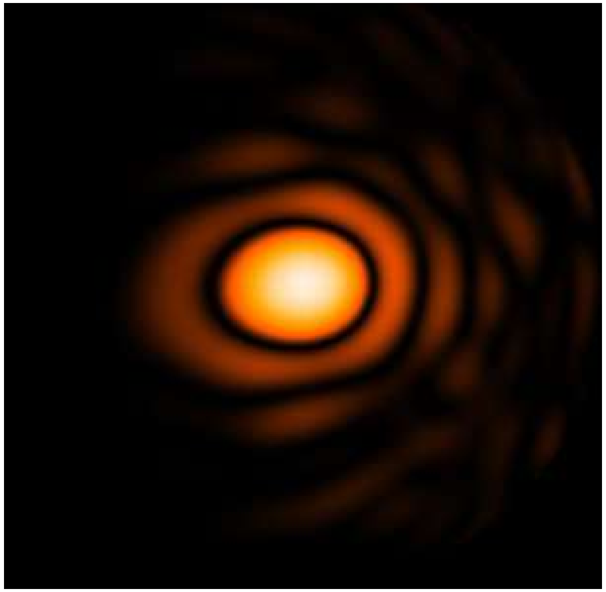

VLA has beam squint

Stokes V

(R – L)

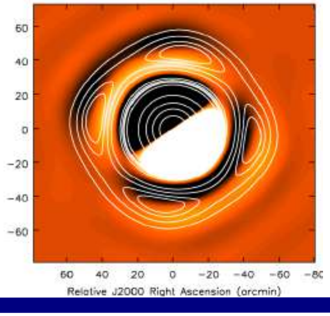

Typically for the ALMA and VLA, errors occur at the 10^4 dynamic range level if such primary beam variations are ignored. Beam squint and pointing offsets cause the dominant errors. For aperture arrays, the shape cannot be ignored.

Primary beams vary within an observation

PB rotates with time, for alt-az mount antennas. (e.g. VLA)

PB varies from antenna to antenna within the array (e.g. ALMA)

PB shape changes with direction on the sky for aperture arrays (e.g. LWA)

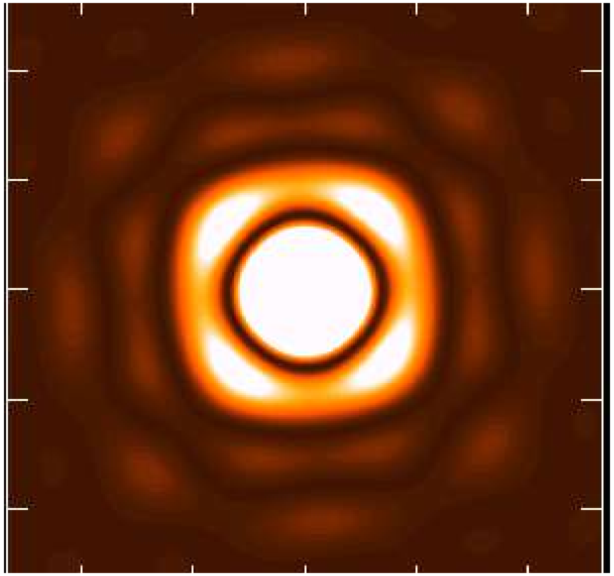

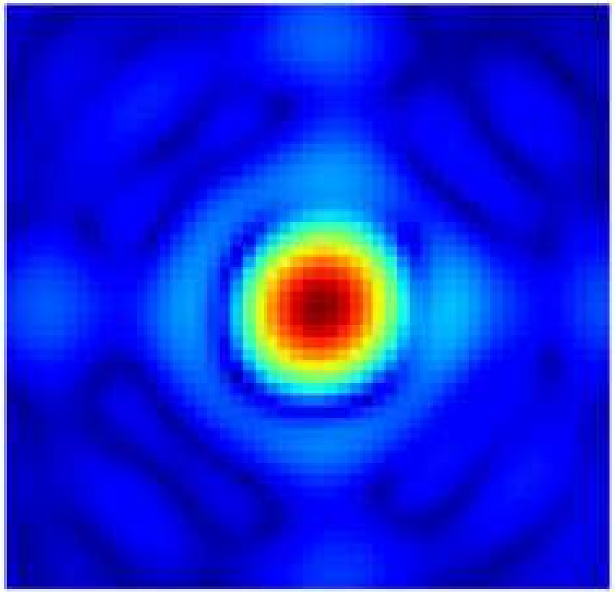

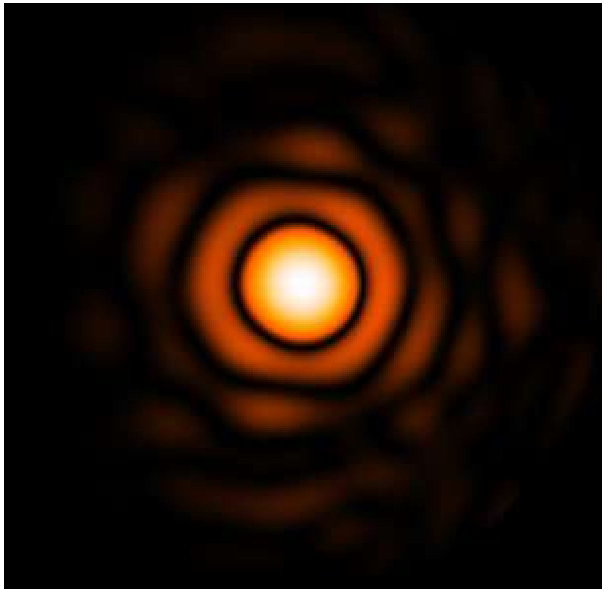

VLA has beam squint

Stokes V

(R – L)

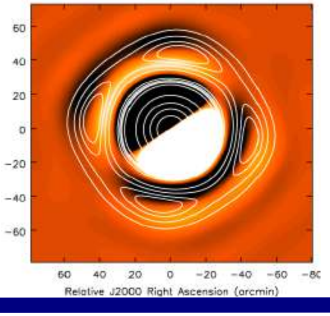

Typically for the ALMA and VLA, errors occur at the 10^4 dynamic range level if such primary beam variations are ignored. Beam squint and pointing offsets cause the dominant errors. For aperture arrays, the shape cannot be ignored.

Primary beams vary within an observation

PB rotates with time, for alt-az mount antennas. (e.g. VLA)

PB varies from antenna to antenna within the array (e.g. ALMA)

PB shape changes with direction on the sky for aperture arrays (e.g. LWA)

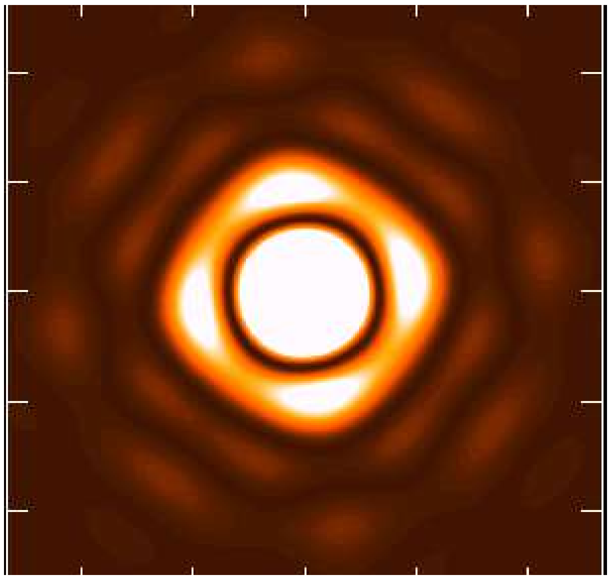

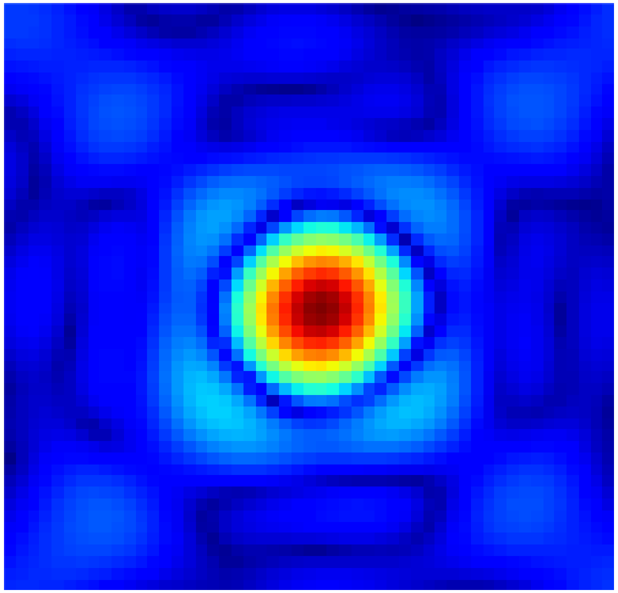

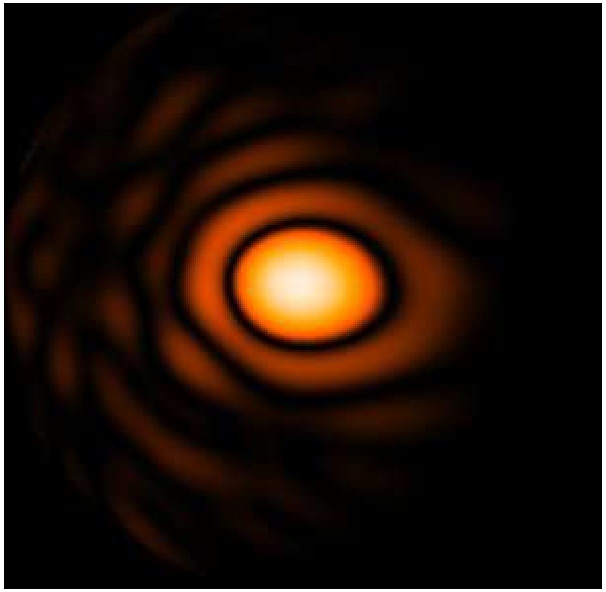

VLA has beam squint

Stokes V

(R – L)

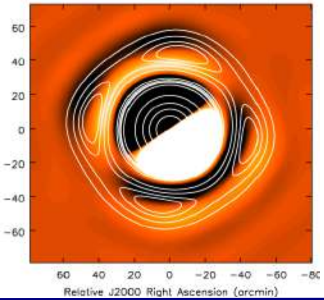

Typically for the ALMA and VLA, errors occur at the 10^4 dynamic range level if such primary beam variations are ignored. Beam squint and pointing offsets cause the dominant errors. For aperture arrays, the shape cannot be ignored.

Primary Beam – Effect on images (VLA sim example)

(1) Multiplicative gain pattern => attenuation away from the center

(2) Variable gain (due to PB variation) => artifacts around bright sources.

$$\delta I^{obs} = \sum_t I^{PSF}(t) * \left[\delta P(t) \cdot I^{sky}\right]$$

Dynamic range of 10^4

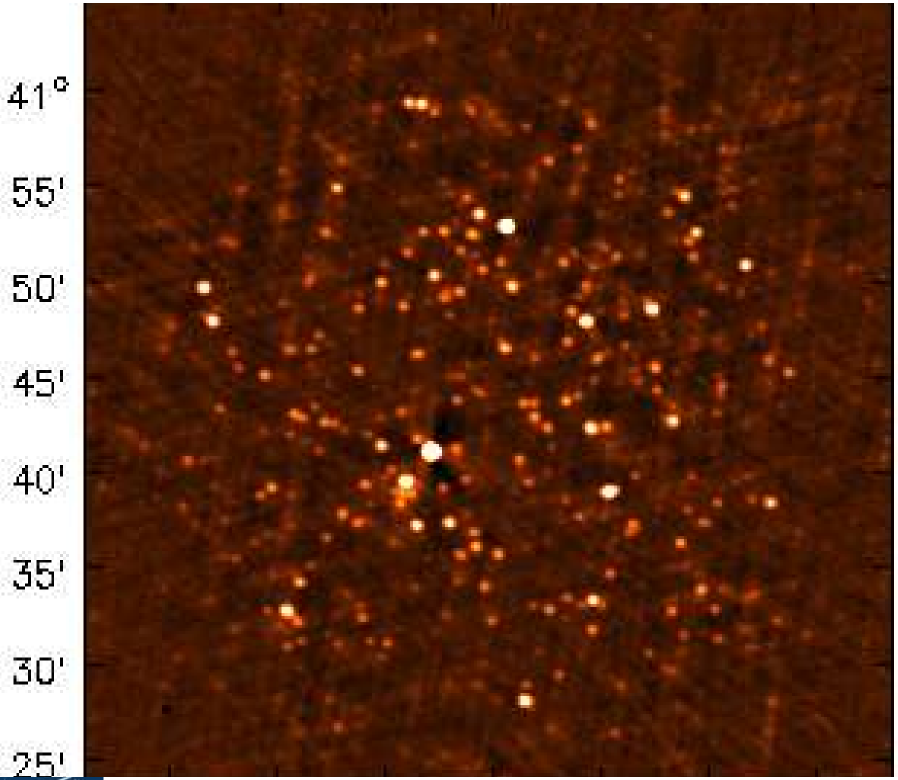

Dynamic range of 10^5

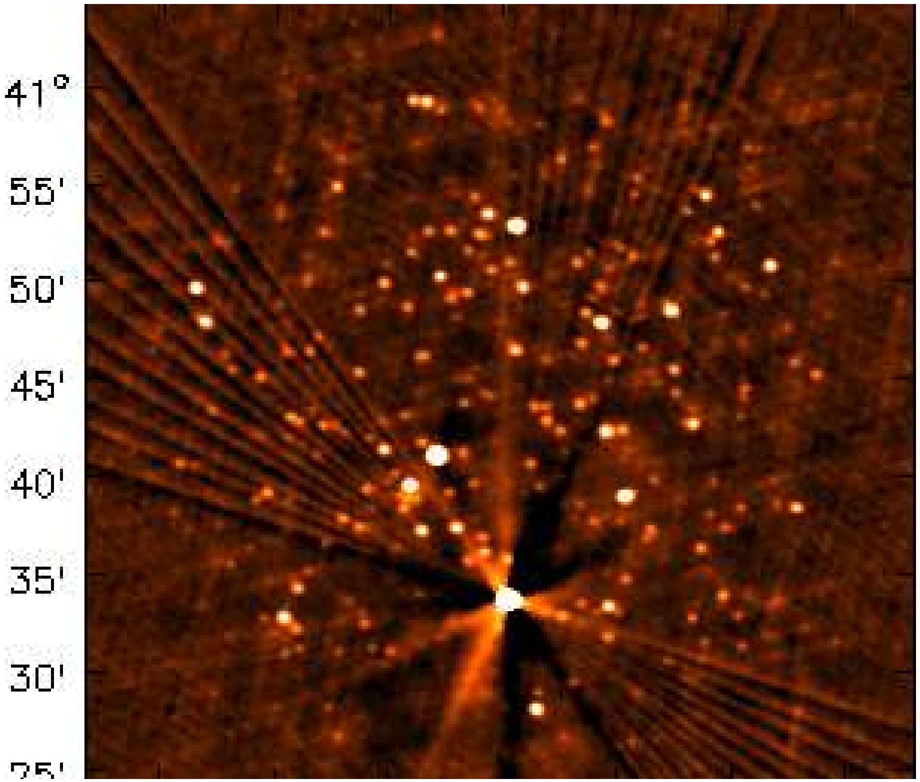

Primary Beam Correction : A-Projection

Bhatnagar et al, 2008

Apply PB correction in the UV-domain **before** visibilities are combined.

$$I_{ij}^{obs} = I_{ij}^{psf} * \left[P_{ij} . I^{sky} \right] \longleftrightarrow V_{ij}^{obs} = S_{ij} . \left[A_{ij} * V^{sky} \right]$$

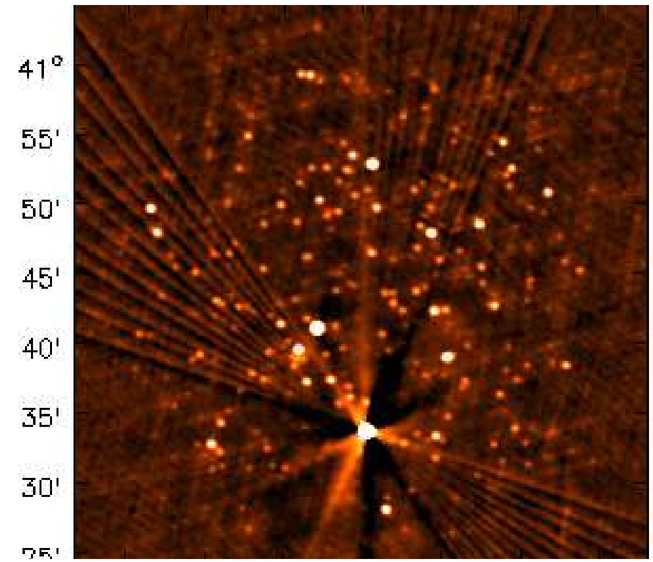

For each visibility, apply $A_{ij}^{-1} \approx \dfrac{A_{ij}^{T}}{A_{ij}^{T} * A_{ij}}$

(1) Use A_{ij}^{T} as the convolution function during gridding

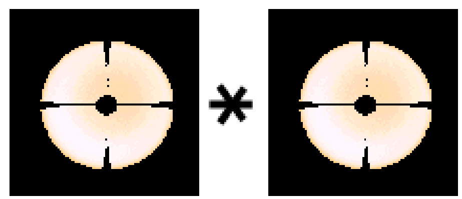

(2) Divide out $FT\left[\sum_{ij} A_{ij}^{T} * A_{ij} \right]$ from the image (in stages).

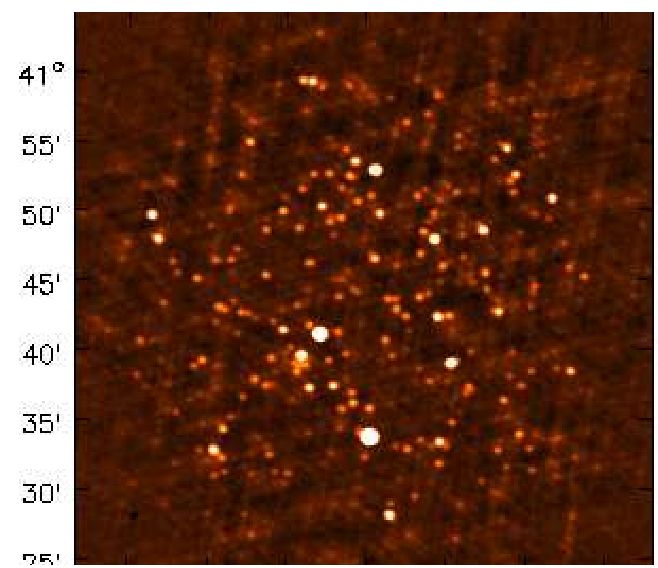

– Conjugate transpose corrects for known pointing offsets such as beam squint.

– An additional phase ramp is applied for different pointings to make a joint mosaic.

Primary Beam – A-Projection on IC2233 field

Images from S.Bhatnagar

Example : Correction of false Stokes-V signal from VLA Beam Squint

Before

After

Stokes I

Artifacts around all sources away from the pointing center

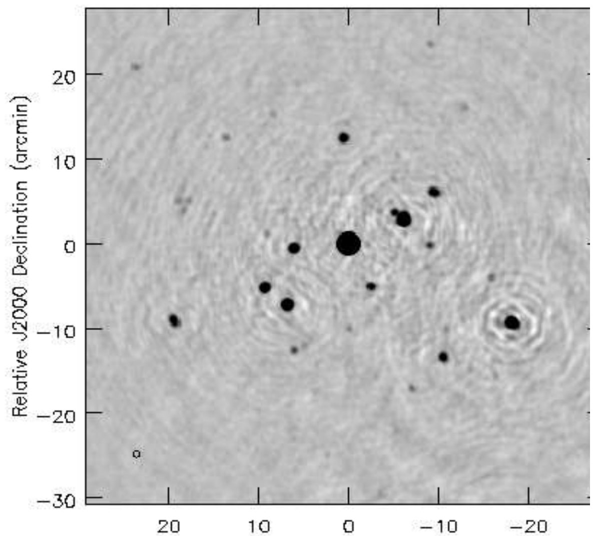

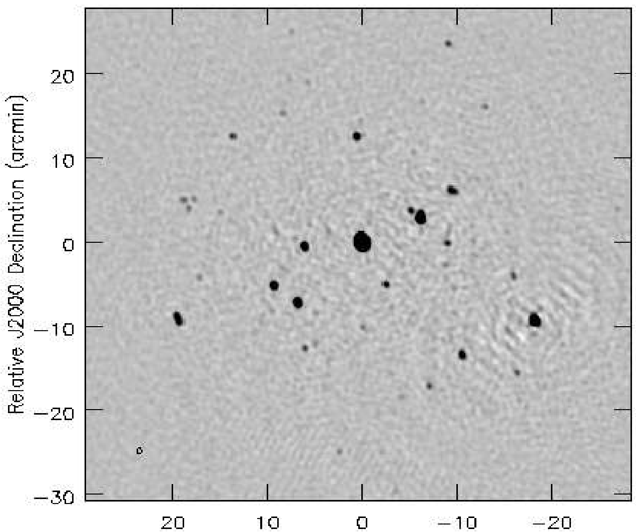

Stokes I

Artifacts removed or reduced within the main lobe

Stokes V

Artificial signals around bright sources due to beam squint

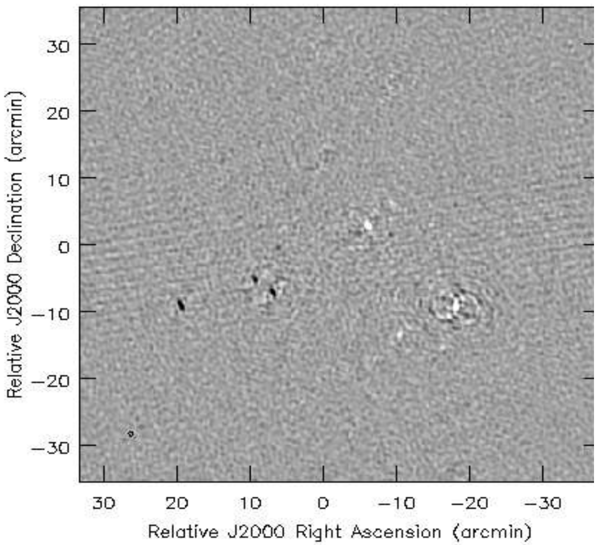

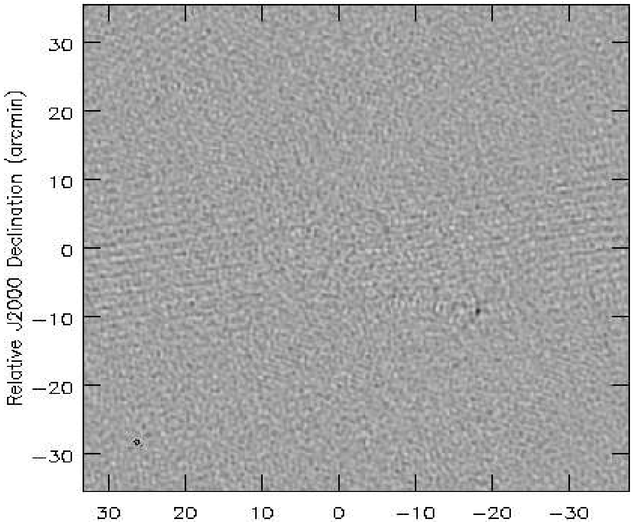

Stokes V

Instrumental Stokes V removed within the main lobe

Accuracy of our PB models outside the main lobe ?

Full-Mueller A-Projection (VLA primary beam model)

Needed for Full Stokes (I,Q,U,V) imaging over the full primary beam

Full polarization primary beams

$$P_{ij}^{RR}, P_{ij}^{LL}, etc$$

Shows the magnitude of direction dependent polarization leakage

PB peak = 1.0
Leakage = 0.001
Source pol = 0.01
=> a 10% effect

A_{ij}^{T} in A-Projection represents the conjugate transpose of the full matrix

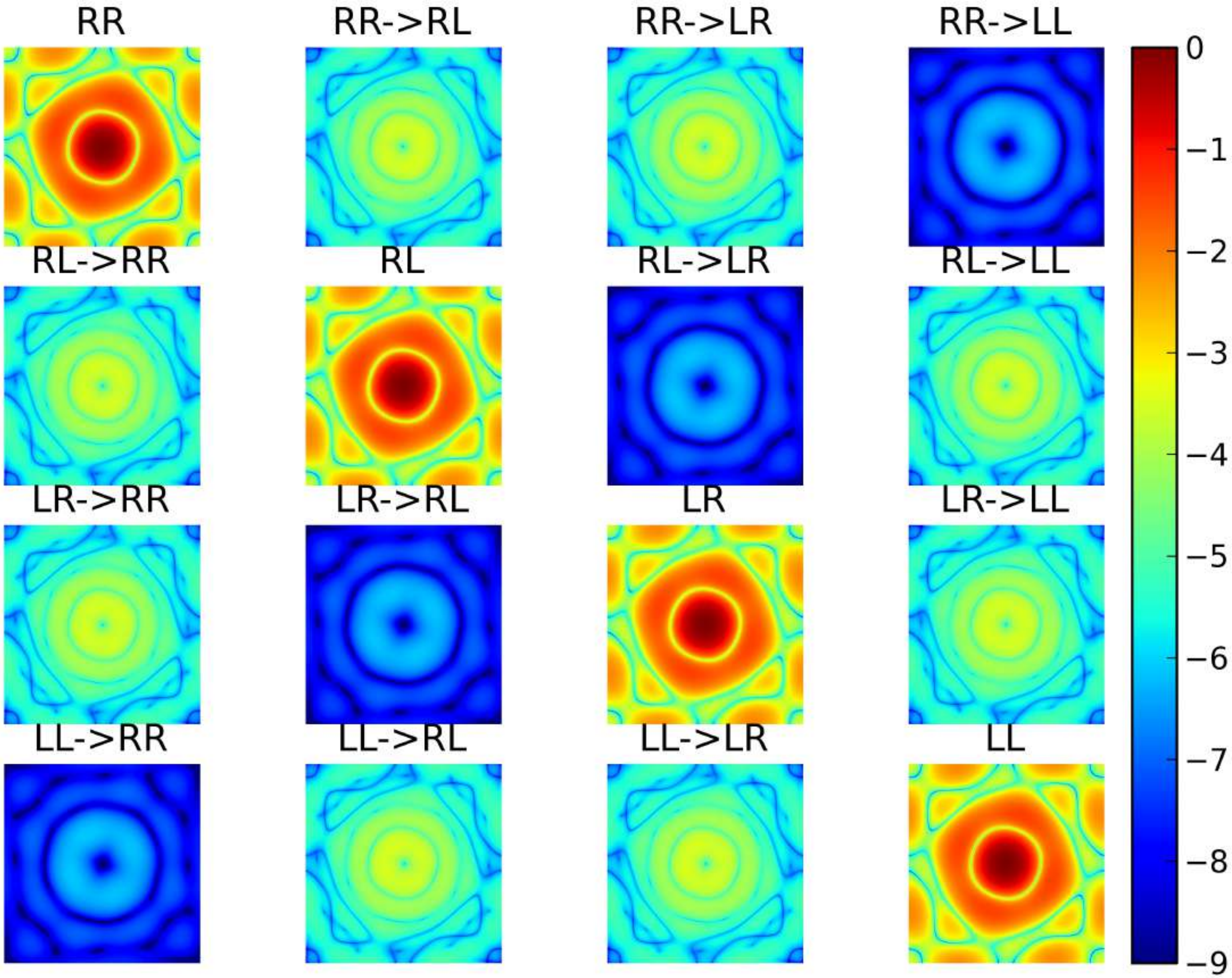

Images from P.Jagannathan

Primary Beam Models – Known / Unknown

Accuracy of PB-correction depends on the quality of the PB model

Several types of PB models are in current use.

(1) Modified Airy disk : Fourier transform of autocorrelation of a (tapered) circular aperture

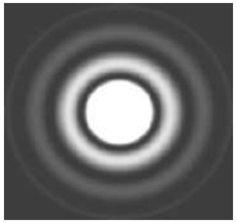

(2) Ray-traced model : Parameterize the dish surface and other structures. Use electromagnetic wave propagation to calculate the aperture illumination function *Brisken, 2011*

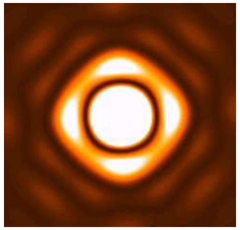

Solve for parameters during imaging : e.g. pointing self-cal *Bhatnagar et al, 2017*

(3) Models derived from measured primary beams (for each antenna/band) :

(a) 1D polynomial fits to azimuthally averaged primary beams *Perley, 2017*

(b) Use measured beams to solve for dish shape parameters and make a ray-traced model *Jagannathan et al, 2017*

(4) Direction dependent self-calibration : No physically motivated PB model
=> Self-cal in multiple directions at once [REF : T.Clarke's talk]

Summary – Lecture I

Factors that break the 2D Fourier relation between the sky model and the measured visibilities + Algorithms to handle them

Wide Band Imaging
Sky and instrument change with frequency
=> Cube vs MFS, wideband/multiscale model, spectral index

Wide Field Imaging
Non-coplanar baselines and the W-term
=> W-Projection, W-Stacking, Faceting, 3D FFTs

Full Beam Imaging
Antenna primary beams
=> pbcor, A-Projection, beam models

Lecture II : Combining all of the above